

The Pennsylvania State University
The Graduate School

PRESCRIPTIVE UNITARITY IN NON-PLANAR THEORY

A Dissertation in
Physics
by
Yaqi Zhang

© 2024 Yaqi Zhang

Submitted in Partial Fulfillment
of the Requirements
for the Degree of

Doctor of Philosophy

May, 2024

The dissertation of Yaqi Zhang was reviewed and approved by the following:

Jacob L. Bourjaily
Associate Professor of Physics
Thesis Advisor
Chair of Committee

Radu Roiban
Professor of Physics

Murat Günaydin
Professor of Physics

Nigel Higson
Evan Pugh Professor of Mathematics

Mauricio Terrones
Professor of Physics
Verne M. Willaman and Evan Pugh Department Head

Abstract

We construct all N^k MHV six-particle amplitude integrands in color-dressed, maximally supersymmetric Yang-Mills theory at two loops in a single prescriptive basis of master integrands. We outline the concrete steps involved in building prescriptive master integrand bases for scattering amplitudes beyond the planar limit. We highlight the role of contour choices in such bases, and illustrate the full process by constructing a complete, triangle power-counting basis at two loops for six particles. We show how collinear contour choices can be used to divide integrand bases into separately finite and divergent subspaces, and how double-poles can be used to further subdivide these spaces according to (transcendental) weight. We prove that all tree-level amplitudes in pure (super-)gravity can be expressed as term-wise, gauge-invariant double-copies of those of pure (super-)Yang-Mills obtained via BCFW recursion. These representations are far from unique: varying the recursive scheme leads to a wide variety of distinct, but equally valid representations of gravitational amplitudes, all realized as double-copies.

Table of Contents

Acknowledgments	vi
List of Tables	vi
Introduction	1
Chapter 1	
Review: Essential Elements of Integrand-Basis Building	7
1.1 Power-Counting of Integrands Beyond the Planar Limit	11
1.2 Non-Planar, Triangle Power-Counting Basis at Two Loops	12
Chapter 2	
Illustrating Implications of Contour-Choices at One Loop	15
2.1 Box Power-Counting Basis and the No-Triangle Property	15
2.2 Possible Choices of Triangle Power-Counting Bases at One Loop	16
2.2.1 Option 1: Exploiting Residues on Poles at Infinity	17
2.2.2 Option 2: Contours Supported in Regions of IR Divergence	19
Chapter 3	
Building a Non-Planar Integrand Basis at Two Loops	21
3.1 Identifying Candidate Numerators and Contours	23
3.2 Step 1. Guessing a Spanning Set of Top-Level Numerators	24
3.3 Step 2. Block-Diagonalization with Respect to a Choice of Contours	27
3.3.1 Requiring the Set of Contours be Graph Symmetric	28
3.3.2 Contours Involving Double-Poles	30
3.4 Step 3. Global Diagonalization of the Basis	32
3.5 Features of the Resulting Basis of Integrands	36
Chapter 4	
Six-Particle N^kMHV Amplitudes at Two-Loops	37
4.1 Summing Terms for Amplitudes	38
4.2 The Six-Particle MHV Amplitude	41
4.3 The Six-Particle NMHV Amplitude	41
4.3.1 Integration, Infrared Structure, and Regularization	42

4.3.2	Consistency Checks	43
Chapter 5		
	Gauge-Invariant Double-Copies via Recursion	44
5.1	Tree-Level, On-Shell Recursion for YM and GR	44
5.2	On-Shell Diagrammatics of YM and GR	46
5.3	Color-Kinematic <i>Denominators</i> for Gravity	47
5.4	Illustrations of On-Shell Double-Copies	48
5.5	Non-Uniqueness of Dual Denominators	50
Chapter 6		
	Conclusions and Future Directions	52
Bibliography		55

Acknowledgments

I extend profound gratitude to my Ph.D. advisor, Professor Jacob Bourjaily, whose unwavering support and guidance empowered me to explore my research interests. His trust allowed me the freedom to navigate the challenges of academic inquiry with confidence. Cameron Langer, the former postdoc, deserves special thanks for his invaluable expertise and collaborative spirit.

Heartfelt thanks go to my research group members, Nikhil Kalyanapuram, Kokkimidis Patatoukos, and Michael Plessner, Cristian Vergu. Their camaraderie and support created an enriching environment for intellectual growth.

I am indebted to my undergraduate advisor, Professor Bowen Xiao, and Professor Anna Stasto, for sparking my passion for high-energy physics. Professor Radu Roiban and Professor Irina Mocioiu contributed significantly to my understanding through their impactful courses.

Appreciation is extended to my dissertation committee members: Professor Nigel Higson, Professor Murat Günaydin. Their constructive feedback refined my research and scholarly contributions.

This project has been supported by an ERC Starting Grant (No. 757978), a grant from the Villum Fonden (No. 15369), by a grant from the US Department of Energy (No. DE-SC00019066). The findings and conclusions of this dissertation do not necessarily reflect the view of the funding agency.

Finally, my deepest gratitude to my parents Ling Zhang and Qingyong Zhang for their unwavering support.

In conclusion, this academic journey has been marked by the generosity, support, and wisdom of many individuals. Each person mentioned has played an integral role in shaping my academic and personal development, and for that, I am sincerely grateful.

List of Tables

1.1	The starting point in our basis construction: the complete list of integrand topologies compatible with triangle power-counting, as defined in [21], reproduced from [31]. Included is the total rank of the vector space of numerators in \mathfrak{B}_3 , as well as the decomposition of these ranks into top-level and contact terms.	13
1.2	Enumeration of the topology distributions and rank-counts for graphs with six external legs. The index ranges are those used to identify integrands in the ancillary files.	14
5.1	On-shell, gauge-invariant contributions to the 6-point NMHV partial amplitudes of Yang-Mills and gravity. The Grassmann $\delta^{3 \times 4}(C_i \cdot \tilde{\eta})$ appearing in these numerators are defined in (5.17).	46
5.3	Alternative recursion schemata resulting in distinct ordered, partial amplitudes $\mathcal{A}^{\text{GR}}(1, 2, 3, 4, 5, 6)$:	49
5.2	Alternative recursion schemata resulting in distinct ordered, partial amplitudes $\mathcal{A}^{\text{GR}}(1, 2, 3, 4, 5)$:	50

Introduction

Recent years have been witness to incredible advances in our understanding of perturbative quantum field theory; much of this has resulted from concrete applications of generalized unitarity: through constructions of specific target amplitudes, matching field theory cuts at the integrand-level. In particular, such investigations [1–3] led to the discovery of tree-level [4, 5] (and loop-level [6]) on-shell recursion relations; the discovery of dual-conformal (and ultimately, Yangian-)invariance [7–10] of planar, maximally supersymmetric Yang-Mills theory; the connection between on-shell diagrams and subspaces of Grassmannian manifolds [11–17]; and the amplituhedron [18–20]—among much else.

Perhaps not surprisingly, the vast majority of this progress has been made in the context of planar theories. For one thing, loop integrands in planar theories can be assigned (symmetrized) dual-momentum coordinates for loop momenta in which all Feynman diagrams depend universally. This allows for *the* loop integrand to correspond to a specific, unambiguous rational function of internal and external (dual) momenta. Moreover, dual coordinates allow a preferential stratification—or organization—of loop integrand bases according to their UV behavior in these coordinates.

Beyond the planar limit, the non-existence of a *particular* rational function has dramatically hindered progress. This is somewhat surprising, because very little about generalized unitarity depends on the coordinates used to describe loop momenta or how momentum-conservation is solved to express an L -loop integrand in terms of some particular choice of loop momenta to be integrated (how the loop momenta are ‘routed’ in the language of ref. [21]). Nevertheless, applications of generalized unitarity beyond the planar limit have been surprisingly sparse. Due to the importance of the possible UV divergence of maximally supersymmetric ($\mathcal{N}=8$) supergravity and the connections between this theory and ($\mathcal{N}=4$) supersymmetric Yang-Mills theory (‘sYM’), the most impressive results that exist are for four-point amplitudes—which are known through five loops [22–29]. Outside of this case, only relatively isolated examples of amplitudes are

known. These include the five and six-point MHV amplitudes in sYM [30, 31] and a more recent, general formula for all-multiplicity MHV amplitudes at two loops [32]. Compare this with planar sYM, for which local integrand representations of all-multiplicity, all N^k MHV amplitudes are known through three loops [33–35], and isolated examples of integrands at lower-multiplicity are known as high as ten loops [36–38].

Interestingly, and in contrast with the work on planar amplitudes, none of the previous applications of generalized unitarity to non-planar amplitudes built upon a *complete* basis of integrands in which to express the result. Rather, all such results were obtained by starting from a reasonably good guess for a *sufficient* subspace of integrands and amending this guess only as far as needed to match the amplitudes in question.

In this work, we would like to take some of the guess-work and cleverness out of the construction of non-planar amplitudes by illustrating the construction of a *complete* and *prescriptive* basis for all (not necessarily planar) integrands with triangle power-counting, (denoted ‘ $\mathfrak{B}_3^{(4)}$ ’ in [21]) involving six particles at two loops, following the general strategy described in ref. [21]. To be clear, although ref. [21] described how to *define* and *enumerate* the space of such integrands beyond the planar limit, it did not discuss how *particular* choices of basis elements should be chosen.

A *prescriptive* basis of integrands $\{\mathcal{I}_i\}$ —viewed as a basis for cohomology on the space of differential forms on loop momenta—is one which is the cohomological dual of some choice of integration contours $\{\Omega_j\}$. That is, a basis of loop integrands $\{\mathcal{I}_i\}$ is called *prescriptive* if there exists a set of cycles $\{\Omega_j\}$ such that

$$\oint_{\Omega_j} \mathcal{I}_i = \delta_{i,j}. \quad (1)$$

When this is the case, amplitudes may be expanded in this basis simply as

$$\mathcal{A} = \sum_i \mathbf{a}_i \mathcal{I}_i \quad (2)$$

with coefficients \mathbf{a}_i being directly (possibly generalized [21, 39]) ‘leading singularities’

$$\mathbf{a}_i := \oint_{\Omega_i} \mathcal{A} \quad (3)$$

—on-shell functions computed in terms of tree-amplitudes.

Obviously, the particular integrands appearing in a prescriptive basis will depend strongly on the integration contours $\{\Omega_j\}$ to which they are dual. One motivation for our

present work is to illustrate the scope of possible choices for these cycles, and how these choices affect the resulting integrand basis in a concrete case of relevance to amplitudes in sYM. For example, by choosing as many contours as possible to encompass all regions responsible for IR-divergence [40], diagonalization of the basis implicit in (1) should render all integrands *not* manifestly dual to such contours IR-finite. Such a splitting of integrands in the basis should simplify the computation of finite quantities (such as the ratio function)—possibly even achieving local finiteness as described in [40]. It remains to be seen how these ideas generalize to beyond the planar limit, and it may be viewed as a conjecture—to be tested by direct integration—that the integrand basis we construct here has this property.

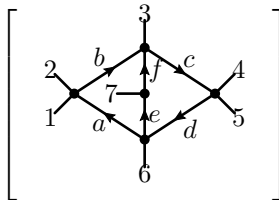
Regardless of the integration contours chosen for the basis, it is empirically the case that prescriptive integrand bases turn out to be ‘simple’ with respect to the difficult challenge of loop integration. Specifically, we mean that they are almost certainly ‘pure’ (at least when maximal in weight) [41, 42]; that is, viewed as master integrals, they are found to satisfy nilpotent systems of differential equations [43, 44]. This property may be complicated by the presence of integrals with double-poles (or equivalently, integrals that should be viewed as maximal in weight for a lower spacetime dimension of integration). The basis we construct certainly includes such integrands; and so it may be viewed as a conjecture—again, to be tested by direct integration—as to whether the full-weight subspace of integrands we construct are indeed ‘pure’ after loop integration.

The existence of integrand basis elements with less than maximal transcendental weight—features widely believed to be absent from amplitudes in sYM—illustrates another motivation for this work: to explore and clarify the ways in which the basis of triangle power-counting integrands ($\mathfrak{B}_3^{(4)}$) as defined in ref. [21] is *too large* for amplitudes in sYM. As we will see, many integration contours can be chosen for which all amplitudes in sYM are known to vanish. In addition to integrands with double-poles, there are many which can be normalized on contours involving poles at infinity—for which amplitudes in sYM are known (at this loop order) or widely expected to vanish [23, 45].

Finally, a practical motivation for this present work is the prospect of constructing a single integrand basis large enough to span all N^k MHV amplitudes in sYM at some fixed multiplicity. Although the six-particle MHV amplitudes at two loops are known in multiple forms [31, 32], the six-point NMHV amplitude remains an important, and open target for investigation. By expressing both amplitudes in the *same* basis of master integrands, there is some hope that it may simplify the work of loop integration for some analogue of the ratio function in the planar case. The analogous results in the planar

limit proved important seeds for future discovery and development [46–49], and we hope this work may inspire some ambitious loop-integrators to take up this challenge once the corresponding amplitudes are known [50].

Let us briefly describe why we have chosen to use the case of non-planar integrands at two-loops involving *six* external particles as the primary example discussed in this work. As discussed at length in [31], six-particle amplitudes are the last multiplicity which can be represented in terms of *manifestly* (and individually) polylogarithmic integrands. In the context of maximal sYM, this can be made obvious by considering the seven-point ‘tardigrade’ topology, whose maximal cut surface has support on an elliptic sub-topology [51],

$$\text{Res}_{a^2=\dots=f^2=0} \left[\begin{array}{c} \text{Diagram} \end{array} \right] \propto \frac{dx}{y}, \quad \text{where } y^2 := Q(x), \quad (4)$$


where $Q(x)$ is an irreducible quartic in the remaining loop variable; as such, this integral involves the geometry of an elliptic curve. Because the integral in (4) has NMHV coloring, *any* representation of the 7-point NMHV amplitude *necessarily* requires terms with support on this elliptic integral. To be clear, although the maximal cut (4) has no further residues on which to define a contour, this presents no fundamental obstacle to defining a spanning set of contours with which to diagonalize numerators. Indeed, the recent works [39, 52] (see also [51, 53–55]) demonstrate that for *any* topology with elliptic (or worse) structures a natural choice of contours may be furnished by some choice of homological cycles within the cut-surface’s geometry. In the above example, these would simply be a choice of either the a - or b -cycle of the elliptic curve.

Another reason we have chosen to focus on the case of six particles is primarily pragmatic: integrals with this multiplicity are (or just beyond) the current state-of-the-art in loop integration. Moreover, a six-point prescriptive basis (in which both the MHV and NMHV amplitudes were expressed) would allow for the direct search of some non-planar analogue of the ratio function beyond the planar limit.

In our basis, all six-particle helicity amplitudes in color-dressed, maximally supersymmetric ($\mathcal{N}=4$) Yang-Mills theory (‘sYM’) or maximal ($\mathcal{N}=8$) supergravity (‘SUGRA’) should be expressible. In this work, we use unitarity to determine the coefficients of all six-particle N^k MHV amplitudes in this basis—of which the NMHV amplitude is entirely new. These coefficients are each simple *leading singularities*, expressible as (fully

color-dressed) on-shell functions, valid for any choice of gauge group.

The rich connections between scattering amplitudes in gauge theory and gravity has been a source of tremendous progress in our understanding of both theories. Among the most seminal of these is so-called color-kinematic (or ‘BCJ’) duality [56], which states that gravitational scattering amplitudes may be represented as ‘double-copies’ of those of Yang-Mills theory, provided the latter is represented in terms of color-kinematic satisfying (‘dual’) numerators with denominators (typically) built from scalar φ^3 field theory (see e.g. [57–60]). The existence of such numerators was first conjectured, but can be proven at tree-level in a number of ways [61–65], with much evidence suggesting that color-kinematic duality should continue to the level of loop integrands (see e.g. [29, 30, 66–74]). The potential form, structure, and scope of these numerators, as well as the theoretical origins of this story more generally have been the subject of a great deal of research (see e.g. [75–81]).

Prior to the discovery of color-kinematic duality, on-shell recursion relations [82–84] for tree-level scattering amplitudes led to similarly great leaps in our understanding of gravitational and gauge-theory amplitudes [85–92]. Some of this work connected directly to results derived from string and twistor string theory (e.g. [93–97]).

In this work, we show that BCFW recursion relations directly lead to representations of amplitudes in color-dressed Yang-Mills theory (YM) and gravity (GR) that may be expressed in the form

$$\begin{aligned} \mathcal{A}^{\text{YM}}(1, \dots, n) &= \sum_{\vec{a} \in \mathfrak{S}(A)} \sum_{\Gamma} \frac{c_{\alpha\beta}^{\vec{a}} n(\Gamma_{\alpha\beta}^{\vec{a}})}{D(\Gamma_{\alpha\beta}^{\vec{a}})} \delta^{2 \times 2}(\lambda, \tilde{\lambda}) \\ \mathcal{A}^{\text{GR}}(1, \dots, n) &= \sum_{\vec{a} \in \mathfrak{S}(A)} \sum_{\Gamma} \frac{n(\Gamma_{\alpha\beta}^{\vec{a}}) n(\Gamma_{\alpha\beta}^{\vec{a}})}{D(\Gamma_{\alpha\beta}^{\vec{a}})} \delta^{2 \times 2}(\lambda, \tilde{\lambda}) \end{aligned} \quad (5)$$

for any choice $\{\alpha, \beta\} \subset [n]$ of the external legs, where $A := [n] \setminus \{\alpha, \beta\}$. For Yang-Mills theory, the form (5) will be seen to be somewhat quixotic, as the color-kinematic dual ‘numerators’ will be simply *defined* to be the product of $D(\Gamma_{\alpha\beta}^{\vec{a}})$ and a more familiar gauge-invariant, on-shell function [98]; as such, the real novelty arises in the identification of the *denominators* $D(\Gamma_{\alpha\beta}^{\vec{a}})$, which we define recursively. It is worth pointing out that because the color-factors appearing in (5) are entirely independent, these numerators are only ‘color-kinematic dual’ in a rather trivial sense: neither satisfies any identities.

The existence of formulae such as (5) follows from the on-shell diagrammatic interpretation of BCFW recursion in YM. Ignoring factors of color and momentum conservation,

the double-copy follows from the fact that for any primitive¹ on-shell diagram Γ , the on-shell functions f_Γ of gravity and Yang-Mills differ by a simple factor depending on the graph:

$$f_\Gamma^{\text{GR}} = J(\Gamma) \left(f_\Gamma^{\text{YM}} \right)^2. \quad (6)$$

This general fact (see e.g. [99–103]) is a simple consequence of the definition of an on-shell function and the relationship between the 3-particle S -matrices of the two theories: an on-shell function may be defined as the product of amplitudes evaluated on the *residue* $1/J(\Gamma)$ of the scalar graph which puts all internal lines on-shell; squaring an on-shell function in YM gives the correct product of 3-particle amplitudes in GR, but squares also $1/J(\Gamma)$ —which must be corrected by the numerator of (6).

This work is organized as follows. In section 1 we review the relevant aspects and benefits of the prescriptive approach to generalized unitarity, as well as the graph-theoretic definition of power-counting for multi-loop integrand bases introduced in [21]. In section 2 we explore the relation between contour choices and the properties of the induced prescriptive integrand bases at one loop, and provide a pedagogical derivation of novel triangle power-counting bases related to the chiral box expansion of [33]. Section 3 contains a thorough outline of the steps involved in constructing prescriptive integrand bases, and the application of these ideas to the case of six particles at two loops. We also discuss desirable features and possible applications of the aforementioned basis, both from the perspective of amplitude integrand construction and for loop integration. Section 4 discusses the application of unitarity to determine the coefficients of all six-particle $N^k\text{MHV}$ amplitudes in this basis. In section 5, we show that BCFW recursion relations directly lead to representations of amplitudes in color-dressed Yang-Mills theory (YM) and gravity (GR) which are related by double copies. Section 6 gives a summary and a discussion of natural directions for further research.

¹A *primitive* diagram is one involving only three-point amplitudes at its vertices. Any diagram with higher-point amplitudes can be expanded as a sum of primitives via BCFW recursion.

Chapter 1 |

Review: Essential Elements of Integrand-Basis Building

Even before we describe the choices involved in making a particular choice for the basis elements of set of loop integrands, it is important to first enumerate the space of integrands under consideration. Typically, this consists of a choice of Feynman integral topologies—defining the propagators of the integrands in the basis—and then some stratum of allowed loop-dependent numerator degrees of freedom. These loop-dependent numerators are usually organized according to some notion of power-counting—limiting the degree of polynomial loop-dependence of the numerators to be considered in the basis.

In [21] it was argued at length that the numerators of any basis are best organized not by Lorentz-invariant scalar products as is more typical, but rather in terms of the *translates* of inverse propagators involving the momentum flowing through some choice of edges of the graph. This choice manifests both the identification of some of these polynomial degrees of freedom as ‘contact terms’ and this organization is naturally translationally invariant—dependent of how the origins of loop momenta are chosen, or how the loop momenta are ‘routed’ through a Feynman graph—how momentum conservation is solved in order to specify some number L independent loop momenta. Thus, this framework organizes loop-dependent numerators in a purely graph-theoretic way.

As this formalism is still somewhat novel, we begin with a rapid but largely self-contained review of the essential ideas and notation introduced in [21] which will be required later in this work.

At one loop, the loop-dependent part of the denominator of any Feynman integrand consists of a single, closed cycle of some number of Feynman propagators. A graph

involving p propagators (and any loop-dependent polynomial in the numerator) is called a ‘ p -gon’. The denominator of a p -gon consists of a product of factors of the form $(\ell|D_i) := (\ell - D_i)^2$; provided the D_i are indexed cyclically around the graph, consecutive D_i ’s differ by the total (external) momentum flowing into a given vertex along the cycle. (Obviously, translation-invariance in ℓ allows us to set any D_i to $\vec{0}$; but it is best if we leave this redundancy in place.)

To describe loop-dependent numerators, we choose (without any loss of generality) to use the same building blocks as the factors appearing in the denominator. Namely, we choose to write any loop-dependent numerator as a polynomial involving products of inverse propagators as monomials. Specifically, we may define

$$[\ell] := \text{span}_Q \{(\ell|Q)\} \quad \text{for } Q \in \mathbb{R}^4. \quad (1.1)$$

That is, $[\ell]$ consists of all polynomials in ℓ that can be written as single inverse propagators with loop-independent coefficients. (These coefficients may depend arbitrarily—typically algebraically—on the external momenta.) It is not hard to see that for four dimensions, $\text{rank}([\ell]) = 6$. Moreover, it is easy to see that this vector space is equivalent to $[\ell] \simeq \text{span}\{1, (\ell \cdot e_i), \ell^2\}$ where e_i are some basis vectors for the space of external momenta, \mathbb{R}^4 . Notice that $[\ell] = [\ell + Q]$ for any $Q \in \mathbb{R}^4$; thus, this is a naturally translationally-invariant notion for a set of loop-dependent numerators.

Higher-order polynomials in ℓ can be constructed as products of inverse propagators. Specifically, we may define

$$[\ell]^q := \text{span}_{\oplus Q_i} \left\{ \prod_{i=1}^q (\ell|Q_i) \right\} \quad \text{for } Q_i \in \mathbb{R}^4. \quad (1.2)$$

It not hard to see that $[\ell]^a \subset [\ell]^b$ for any $a < b$. In particular, $[\ell]^0 = \{1\} \subset [\ell]$, as seen above. These spaces form symmetric, traceless products of 6-dimensional representations of SO_6 —a fact that is easy to see in the embedding formalism (see e.g. [104]). For this work, we will mostly be interested in spaces $[\ell]^0, [\ell]^1, [\ell]^2, [\ell]^3$, which have ranks 1, 6, 20, and 50, respectively.

We can discuss the space of loop-dependent numerators assigned to a given set of Feynman propagators using the following graphical notation:

$$\text{---} \overset{\circ}{\underset{\ell}{\curvearrowright}} \text{---} := \frac{[\ell]}{\ell^2} \simeq \text{span} \left\{ \frac{1}{\ell^2}, \frac{\ell^i}{\ell^2}, 1 \right\}. \quad (1.3)$$

(Notice that this space is large enough to include the propagators of scalars, fermions, and vector bosons (in any gauge).) To illustrate how this notation can be used, consider the space of box integrands with triangle power-counting:

$$\frac{[\ell]}{(\ell|D_1)(\ell|D_2)(\ell|D_3)(\ell|D_4)} \leftrightarrow \begin{array}{c} P_2 \nearrow \quad \searrow P_3 \\ \bullet \quad \bullet \\ \bullet \quad \bullet \\ P_1 \nwarrow \quad \nearrow P_4 \end{array} \quad (1.4)$$

(Momentum conservation requires, for example, that $D_2 - D_1 = P_1$; but to specify the D 's would require that we eliminate the translational-invariance of the loop momentum—something we'd like to avoid.) Because the space $[\ell]$ is invariant under translations, decorating any pair of propagators whose momenta differ by some sum of external momenta would result in the same vector space of loop-dependent numerators; in particular, the decoration on the top edge in (1.4) can be placed on any edge of the graph and would define precisely the same set of Feynman-like loop integrands.

Notice that any element of the space of integrands in (1.4) scales *manifestly* like a scalar triangle integral as $\ell \rightarrow \infty$. Because of this, we describe this space of box integrands in (1.4) as those with ‘triangle’ power-counting.

It is natural to partition the space of loop-dependent numerators as much as possible into ‘contact-terms’—monomials which eliminate one (or more) of the propagators of the graph. In the case of the box in (1.4), the space of contact terms are obviously $\text{span}\{(\ell|D_1), (\ell|D_2), (\ell|D_3), (\ell|D_4)\} \subset [\ell]$. The space of numerators *not spanned by* contact terms is called the numerator’s *top-level* degrees of freedom. This space can be spanned by $\{(\ell|Q^i)\}$ for $i=1,2$ where Q^i represents one of the solutions to the ‘quad-cut’ equation $(Q^i|D_1) = (Q^i|D_2) = (Q^i|D_3) = (Q^i|D_4) = 0$.

Thus, any particular numerator for a box with ‘triangle’ power-counting—any element of (1.4)—could be expressed by

$$[\ell] \ni \mathbf{n}(\ell) =: \underbrace{c^1(\ell|Q^1) + c^2(\ell|Q^2)}_{\text{top-level}} + \underbrace{c^3(\ell|P_1) + \dots + c^6(\ell|P_4)}_{\text{contact terms}} \quad (1.5)$$

where the coefficients $\{c^i\}_{i=1,\dots,6}$ are some ℓ -independent ‘constants’ (arbitrary functions of the external momenta). We would say that a box integral with triangle power-counting’s six-dimensional space of numerators consists of 2 ‘top-level’ degrees of freedom and 4 ‘contact-terms’.

In four dimensions, it turns out that any pentagon (or higher) with triangle power-counting can be expanded into the boxes (1.4) and scalar triangle integrands. Thus, the

complete basis of one-loop integrands with triangle power-counting would be given by

$$\begin{aligned} \mathfrak{B}_3^{(4),L=1} &:= \text{span}_{\oplus D_i} \left\{ \frac{1}{(\ell|D_1)(\ell|D_2)(\ell|D_3)}, \frac{[\ell]}{(\ell|D_1)(\ell|D_2)(\ell|D_3)(\ell|D_4)} \right\} \\ &= \text{span}_{\oplus P_i} \left\{ \begin{array}{c} P_2 \\ \triangle \\ P_1 \quad P_3 \end{array}, \begin{array}{c} P_2 \quad P_3 \\ \square \\ P_1 \quad P_4 \end{array} \right\}. \end{aligned} \quad (1.6)$$

To specify a *particular* basis for this space, both top-level and contact-term degrees of freedom must be defined for every integrand in the basis. It may seem tempting to simply set all contact-terms to zero in the space of numerators, but this is not obviously in line with prescriptivity (1); rather, in any prescriptive basis the contact terms of the boxes are uniquely fixed by the requirement that the box integrands in the basis *vanish on the contours to which the triangles are dual*. Provided any contour used for diagonalization includes ‘cutting’ of every propagator of the integrand, all triangle integrands will automatically vanish on any contour defining a box integrand. This is an illustration of the upper-triangular nature of bases with $< d$ -gon power-counting in d dimensions—something we will discuss in more detail below.

At two-loops (or higher), loop-dependent numerators are organized in a similar way. Before we discuss this, it is worthwhile to review the possible loop dependence in the denominator of any two-loop Feynman graph. Any such graph can be labelled by three numbers, $\{a, b, c\}$ which indicate the number of propagators that are related by translates involving only external momenta; we can see this graphically by describing the denominator of any two-loop integrand as

$$\Gamma_{[a,b,c]} \Leftrightarrow \begin{array}{c} \left. \begin{array}{c} \bullet \\ \bullet \\ \bullet \end{array} \right\} a \\ \left. \begin{array}{c} \bullet \\ \bullet \\ \bullet \end{array} \right\} b \\ \left. \begin{array}{c} \bullet \\ \bullet \\ \bullet \end{array} \right\} c \end{array} \quad (1.7)$$

When discussing loop-dependent numerators for such integrands, we may use inverse propagators involving translates of the momenta flowing through the edges each type in the graph:

$$\begin{aligned} [\ell_A] &:= \text{span}_Q \{(\ell_A|Q)\}, \\ [\ell_B] &:= \text{span}_R \{(\ell_B|R)\}, \quad \text{where } Q, R, S \in \mathbb{R}^4, \\ [\ell_C] &:= \text{span}_S \{(\ell_C|S)\}, \end{aligned} \quad (1.8)$$

as well as (sums of) products thereof. Of course, $[\ell_B] \simeq [\ell_A - \ell_C]$; but as before, we choose to avoid making any choice of loop-momentum routing in order to eliminate one of the three labels.

For any choice of numerators constructed in this way, there will be a natural decomposition into **top-level** degrees of freedom and contact terms. But to specify a particular *set* of such numerators (even before we discuss choosing *particular* representative integrands to span that set) requires that we make some choice of *which* numerators to include for each topology in the basis. Complicating matters is the fact that for non-planar graphs the naïve notion of ‘scaling like a p -gon’ as $\ell \rightarrow \infty$ depends strongly on how the loop momenta are routed—which two cycles of unfixed, internal loop momenta are considered as independent. A proposal for a space of triangle power-counting integrands at any loop order for non-planar graphs was defined in ref. [21], which we review presently.

1.1 Power-Counting of Integrands Beyond the Planar Limit

The essential idea behind the graph-theoretic definition of power-counting described in ref. [21] is that when spaces of loop-dependent numerators are constructed using (1.3) it is clear how every integrand in this space behaves as the loop momentum through any edge goes to infinity: like a constant. That is, putting a decoration as in (1.3) on any edge of a graph results in a space of integrands that scales exactly like the Feynman integrand where all decorated-edges have collapsed.

Thus, while there may be no invariant notion of how a Feynman integrand scales at ‘infinity’ without specifying a particular routing of loop momenta, there is an invariant sense in which one loop integrand can scale like one (or more) among its *contact-terms*. Thus, the starting point for defining \mathfrak{B}_p —the space of integrands with ‘ p -gon’ power-counting—beyond one loop is a specification of which integrands in the basis should be defined as ‘scalars’—those integrands with loop-independent numerators, like which every other integrand in the basis scales at infinity.

Given any choice of ‘scalar’ Feynman graphs, a complete space of integrands which scale like these may be constructed by adding decorated edges (1.3) to these. In any fixed spacetime dimension, there is an upper bound on the number of edges that can be added before the rank of that graph’s top-level degrees of freedom vanishes.

The authors of [21] defined the set of p -gon scalars as any graph with girth p which

would be lowered by the collapse of any edge. At two loops, these scalar 3-gons are defined to be

$$\mathfrak{S}_3 := \left\{ \begin{array}{c} \text{Diagram 1} \\ \text{Diagram 2} \end{array} \right\}. \quad (1.9)$$

From these, the basis \mathfrak{B}_3 would be generated by adding any number of decorated edges (1.3) to either of these graphs (without increasing the loop number). Said another way, any graph that contains either of (1.9) as a contact term would be endowed with a vector-space of numerators given by the product of the translates of inverse propagators corresponding to each edge in the quotient of the parent relative to the daughter. For graphs where more than one edge-sets exists, the space of numerators is defined as the outer-sum of the vector-spaces generated by each.

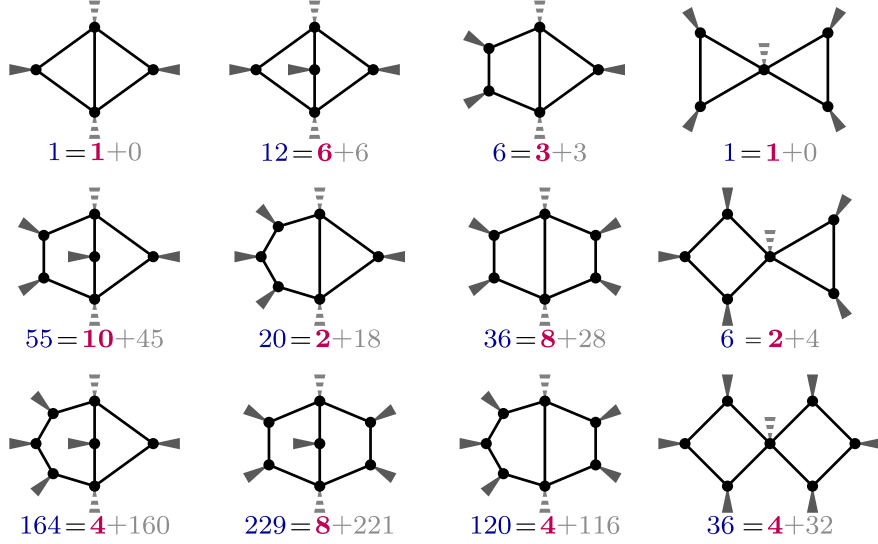
1.2 Non-Planar, Triangle Power-Counting Basis at Two Loops

The set of triangle power-counting integrands consists of all graphs which scale like one or the other of (1.9). In any fixed spacetime dimension (or equivalently, external multiplicity), the space of such integrands is in fact finite dimensional: all but a finite number of integrands with a bounded number of propagators is *reducible*—meaning that its numerator space would entirely spanned by contact terms (its **top-level** rank would be zero).

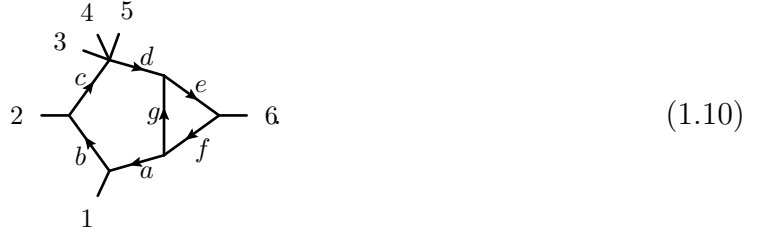
In four dimensions, any integrand with more than eight propagators is reducible in \mathfrak{B}_3 , and those integrands with precisely eight propagators will have precisely as many **top-level** degrees of freedom as there are solutions to the maximal-cut equations (defining contours which ‘encircle’ all of the propagators of the graph). The complete space of such integrands was described in some detail in [21], which is summarized in table 1.1.

In the case of six external particles, the integrands in table 1.1 involve 94 distinct (graph non-isomorphic) instances of distinct leg distributions. Among these, we have

Table 1.1: The starting point in our basis construction: the complete list of integrand topologies compatible with triangle power-counting, as defined in [21], reproduced from [31]. Included is the **total rank** of the vector space of numerators in \mathfrak{B}_3 , as well as the decomposition of these ranks into **top-level** and contact terms.



chosen to disregard 7 of which include massless-triangle sub-topologies—for example,



Such integrands are problematic from a unitarity point of view for the simple reason that when the internal propagators flowing into the massless triangle (a and d above) and any two within the triangle (e , f , and g above) are cut, the third propagator of the triangle will automatically be on-shell (in four dimensions). Thus, the five propagators involved in a massless triangle do give rise to a co-dimension 5, transverse residue. This technical problem can be easily resolved by considering the propagators as massive, for example; but as such integrands form a closed subspace under edge contractions (no integrand *without* a massless triangle has one as a contact term) and as their coefficients would always vanish in sYM, we have chosen to ignore them in our classification.

Thus, including all non-graph-isomorphic leg distributions, and excluding any graphs with massless triangles, we find 87 distinct integrand topologies for six external particles at two loops. We summarize the basis that results in table 1.2.

In total, we have 87 six-particle, two-loop integrand topologies spanning a space of

Table 1.2: Enumeration of the topology distributions and rank-counts for graphs with six external legs. The index ranges are those used to identify integrands in the ancillary files.

topology	#	index range	\mathfrak{N}_3	total rank = top-level rank + contact-terms
$\Gamma_{[4,0,4]}$	1	[1]	$[\ell_A][\ell_C]$	36 = 4 + 32
$\Gamma_{[4,1,3]}$	4	[2-5]	$[\ell_A]^2[\ell_C] \oplus [\ell_A][\ell_B]$	120 = 4 + 116
$\Gamma_{[4,2,2]}$	4	[6-9]	$[\ell_A]^3 \oplus [\ell_A]^2[\ell_C] \oplus [\ell_A]^2[\ell_B]$	164 = 4 + 160
$\Gamma_{[3,2,3]}$	3	[10-12]	$[\ell_B]^2 \oplus [\ell_A]^2[\ell_C] \oplus [\ell_A]^2[\ell_B] \oplus [\ell_A][\ell_B][\ell_C]$	229 = 8 + 221
$\Gamma_{[3,0,4]}$	4	[13-16]	$[\ell_C]$	6 = 2 + 4
$\Gamma_{[3,1,3]}$	8	[17-24]	$[\ell_B] \oplus [\ell_A][\ell_C]$	36 = 8 + 28
$\Gamma_{[4,1,2]}$	9	[25-33]	$[\ell_A]^2$	20 = 2 + 18
$\Gamma_{[3,2,2]}$	10	[34-43]	$[\ell_A]^2 \oplus [\ell_A][\ell_C] \oplus [\ell_A][\ell_B]$	55 = 10 + 45
$\Gamma_{[3,1,2]}$	17	[44-60]	$[\ell_A]$	6 = 3 + 3
$\Gamma_{[2,2,2]}$	9	[61-69]	$[\ell_A] \oplus [\ell_B] \oplus [\ell_C]$	12 = 6 + 6
$\Gamma_{[3,0,3]}$	5	[70-74]	1	1 = 1 + 0
$\Gamma_{[2,1,2]}$	13	[75-87]	1	1 = 1 + 0

373 top-level degrees of freedom (3129 degrees of freedom in total). This is the number of contours which must be specified to define a prescriptive basis. All 3129 degrees of freedom will be fixed by these contours, together with their graph-isomorphic images as contact-term conditions according to (1).

We will return to the details of this integrand basis in section 3; but first, let us briefly return to one loop in order to better understand role of contour choices in the prescriptivity condition (1).

Chapter 2 | Illustrating Implications of Contour-Choices at One Loop

Generalized unitarity at one loop has a long and rich history [1–3, 105–109], and its many refinements have yielded many practical and theoretical discoveries [4, 5, 7–9, 15]. Examples of pedagogical reviews of this material can be found in [110–112] as well as in recent, related works by some of the authors [21, 31, 35]. Before proceeding to the main two-loop results of this paper, in this section we shall take a detour to re-analyze one-loop bases with box and triangle-power counting, with a particular focus on the relation between the contour choices and the properties of the associated bases. In addition to providing some simple examples of the kinds of contour prescriptions we use throughout this work, the main results of this section are two different and novel triangle-power-counting bases which are related to—but slightly different than—the ‘chiral box’ expansion of [33].

2.1 Box Power-Counting Basis and the No-Triangle Property

The standard lore of one-loop generalized unitarity in maximally supersymmetric Yang-Mills (sYM) is that, because amplitudes scale as $\sim (\ell^2)^{-4}$ as $\ell \rightarrow \infty$, a natural choice of power-counting is ‘4-gon’, which in four dimensions consists of scalar boxes and pentagons with a single loop-momentum numerator insertion:

$$\mathfrak{B}_4 \leftrightarrow \left\{ \text{box}, \text{pentagon} \right\}. \quad (2.1)$$


The numerator space for the pentagons is conveniently described in a basis of the five inverse propagators of the graph, plus a single top-level numerator in the complement of that subspace. As every topology has a single **top-level** degree of freedom, the contour prescriptions of this part of the basis are simple: every box may be normalized to be unit on the parity-even combination (the difference of residues) of its respective quad-cuts $f_{A,B,C,D}^{1,2}$, which we may denote diagrammatically as

$$\frac{1}{2} \left(\text{diag}_1 + \text{diag}_2 \right) \leftrightarrow \text{diag}_3, \quad (2.2)$$

while each pentagon can be normalized on a parity-odd contour which results in integrands which integrate to zero. As has been discussed at length in [35], this basis is unfortunately over-complete because the parity-odd pentagons are not all independent: the $\binom{n}{5}$ pentagons satisfy $\binom{n-1}{5}$ linear relations. Eliminating the resulting redundancy requires an (arbitrary) choice of an independent subset of pentagons. This choice, while not a significant roadblock at one loop—especially if one were only interested in integrated expressions—becomes substantially more problematic at higher loops. Fortunately, considering a basis with triangle power-counting is an elegant way of resolving this issue, at the cost of losing manifest dual conformal invariance in the planar part of the basis.

2.2 Possible Choices of Triangle Power-Counting Bases at One Loop

The box power-counting basis of the previous subsection is perfectly natural for representing all one-loop amplitudes in sYM *post-integration*. However, integrand-level representations of these amplitudes require an arbitrary choice of an independent set of parity-odd pentagons. This led to the development of the ‘upgraded’ basis of [33] resulting in the ‘chiral box’ expansion, which made use of a particular, prescriptive basis of triangle power-counting integrands, cleanly separated into infrared finite and divergent subsets. These integrands were designed to have support on one solution to the box-cut, and vanish on the other. In addition, they were designed to vanish on the *parity-even* contour (including infinity) of any *three-mass* triangle sub-topology and on any soft and/or collinear region of any triangle with a massless corner. Thus, the ‘chiral box’ basis described in [33], while not adequately described in these terms, corresponded to a prescriptive basis with the following choice of contours: chiral box-cut contours for each

box integrand; soft and/or collinear regions and parity-even at infinity for all divergent or finite triangle integrals, respectively.

To clarify the role of the contour choices involved, it is worthwhile to revisit the question of triangle power-counting at one loop and derive two new prescriptive bases based upon slightly different contour choices.

2.2.1 Option 1: Exploiting Residues on Poles at Infinity

In a basis with triangle power-counting in four dimensions, every scalar triangle integral has one simple pole at infinite loop momentum along each triple-cut. Thus, a natural choice for their contours would be the parity-even combination of these (which is the difference of the two contours), resulting in a normalization of the integrands given by

$$\begin{array}{c} B \\ \blacktriangledown \\ \bullet \\ \blacktriangledown \\ A \quad \bullet \quad C \end{array} \leftrightarrow \mathbf{n}_{A,B,C} := \frac{1}{2} \sqrt{(p_C^2 - p_A^2 - p_B^2)^2 - 4p_A^2 p_B^2}. \quad (2.3)$$

This normalization smoothly degenerates to all cases involving massless external momenta (the argument of the square root becoming a perfect square for all such degenerations).

As amplitudes in sYM (and SUGRA) have no support on poles at infinity at one loop, the coefficient of any all scalar triangle integrand for amplitudes in sYM will be zero. (This is much more in line with the original observation leading to the ‘no triangle’ hypothesis for these theories [113–118].)

What about the box integral contours? Rather than taking the chiral solutions to the quad-cuts, let’s use the parity-even and parity-odd combinations of contours—that is, the difference and sum of the chiral contours, respectively. Even before we discuss the numerators that result from this choice of contours, it is interesting to note that in the representation of a loop integrand, we would have coefficients arranged according to

$$\frac{1}{2} \left(\begin{array}{c} \circ \quad \circ \\ | \quad | \\ \circ \quad \circ \\ | \quad | \\ \circ \quad \circ \end{array} + \begin{array}{c} \circ \quad \circ \\ | \quad | \\ \circ \quad \circ \\ | \quad | \\ \circ \quad \circ \end{array} \right) \leftrightarrow \begin{array}{c} \circ \quad \circ \\ | \quad | \\ \circ \quad \circ \\ | \quad | \\ \circ \quad \circ \end{array} \text{e}, \quad (2.4)$$

$$\frac{1}{2} \left(\begin{array}{c} \circ \quad \circ \\ | \quad | \\ \circ \quad \circ \\ | \quad | \\ \circ \quad \circ \end{array} - \begin{array}{c} \circ \quad \circ \\ | \quad | \\ \circ \quad \circ \\ | \quad | \\ \circ \quad \circ \end{array} \right) \leftrightarrow \begin{array}{c} \circ \quad \circ \\ | \quad | \\ \circ \quad \circ \\ | \quad | \\ \circ \quad \circ \end{array} \text{o}. \quad (2.5)$$

For the parity-even contour, a loop-independent ‘scalar’ box is an obvious candidate numerator—and obviously an element of \mathfrak{B}_3 (as $\mathfrak{B}_3 \supset \mathfrak{B}_4$). Moreover, the scalar box integral is free of any poles at infinite loop momentum, making them automatically vanish on the contours defining the scalar triangle integrands.

For the parity-odd contours for the boxes, it is clear that we must choose integrands that have equal residues on the two box-cuts so that these integrals vanish on the even-contours (so that the 2×2 system of top-level numerators for each box is diagonal). It turns out to be fairly easy to guess such numerators—which turn out to vanish automatically on all parity-even contours defining all triangle daughter topologies (contact terms).

The final set of numerators will be

$$\mathcal{I}_{A,B,C,D}^{e,o} \leftrightarrow \begin{array}{c} \begin{array}{ccc} & B & \\ & \nearrow c \searrow & \\ b & & d \\ \nwarrow a \nearrow & & \\ & A & D \end{array} \end{array} \leftrightarrow \begin{cases} \mathbf{n}_{A,B,C,D}^e := \frac{1}{2} \sqrt{(p_{AB}^2 p_{BC}^2 - p_A^2 p_C^2 - p_B^2 p_D^2)^2 - 4 p_A^2 p_B^2 p_C^2 p_D^2} \\ \mathbf{n}_{A,B,C,D}^o := \frac{1}{2} (\llbracket p_A, b, c, p_C \rrbracket - \llbracket b, c, p_C, p_A \rrbracket) \end{cases} \quad (2.6)$$

(Here we use the kinematic bracket conventions from [31, 32] to denote contractions of momenta

$$\llbracket a_1, a_2, \dots, c_1, c_2 \rrbracket := \left[(a_1 \cdot a_2)^\alpha_\beta \cdots (c_1 \cdot c_2)^\gamma_\alpha \right], \quad (2.7)$$

where $(a_1 \cdot a_2)^\alpha_\beta := a_1^{\alpha\dot{\alpha}} \epsilon_{\dot{\alpha}\dot{\gamma}} a_2^{\dot{\gamma}\gamma} \epsilon_{\gamma\beta}$ and $a^{\alpha\dot{\alpha}} := a^\mu \sigma_\mu^{\alpha\dot{\alpha}}$ are ‘ 2×2 ’ four-momenta, defined via the Pauli matrices. The ‘ $\llbracket \dots \rrbracket$ ’ object may be more familiar to some readers if written equivalently as ‘ $\text{tr}_+[\dots]$ ’.) Both of these numerators smoothly degenerate under all massless limits of the corners. It is not hard to check that the entire basis is diagonal in the choice of contours described—and is hence *prescriptive*.

Notice that this basis is complete and not over-complete. Thus, the odd numerators for the box integrands are full-rank. Thus, considering that $\mathfrak{B}_3 \supset \mathfrak{B}_4$, although each of these integrands scale like scalar triangle integral at infinite loop momentum, it is interesting to note that all parity-odd pentagon integrands are in fact spanned by these ‘parity-odd’ boxes. This fact is further emphasized by the form that amplitudes take in this basis. For theories with maximal supersymmetry (which have box power-counting, and hence are expressible within \mathfrak{B}_4), amplitudes will take the form

$$\mathcal{A} = \sum_{A,B,C,D} \frac{1}{2} (f_{A,B,C,D}^1 + f_{A,B,C,D}^2) \mathcal{I}_{A,B,C,D}^e + \frac{1}{2} (f_{A,B,C,D}^1 - f_{A,B,C,D}^2) \mathcal{I}_{A,B,C,D}^o \quad (2.8)$$

$$= \sum_{A,B,C,D} \frac{1}{2} \left(\begin{array}{c} \text{---} \circ \text{---} \\ | \quad | \\ \text{---} \circ \text{---} \end{array} + \begin{array}{c} \text{---} \circ \text{---} \\ | \quad | \\ \text{---} \circ \text{---} \end{array} \right) \times \begin{array}{c} \text{---} \circ \text{---} \\ | \quad | \\ \text{---} \circ \text{---} \end{array} + \frac{1}{2} \left(\begin{array}{c} \text{---} \circ \text{---} \\ | \quad | \\ \text{---} \circ \text{---} \end{array} - \begin{array}{c} \text{---} \circ \text{---} \\ | \quad | \\ \text{---} \circ \text{---} \end{array} \right) \times \begin{array}{c} \text{---} \circ \text{---} \\ | \quad | \\ \text{---} \circ \text{---} \end{array}. \quad (2.9)$$

As far as integrals are concerned, this is essentially identical to the representation in \mathfrak{B}_4 —namely, the only integrands that contribute upon integration are the scalar boxes $\mathcal{I}_{A,B,C,D}^e$.

One disadvantage of this choice of contours, however, is that the IR structure of amplitudes is far from manifest: any scalar box with a massless leg will be IR divergent,

and it is a non-trivial fact (an identity that led to the discovery of tree-level recursion relations for amplitudes, in fact [83]) that the total IR divergence of an amplitude would be proportional to the tree.

2.2.2 Option 2: Contours Supported in Regions of IR Divergence

Rather than choosing contours at infinity for all the triangles, let us now consider choosing contours that (in addition to cutting all three propagators) enclose any soft and/or collinear region that may exist. These are the regions in loop-momentum space responsible for IR-divergences [40].

This difference has very little effect on the triangle integrands (whose normalization changes merely by a sign—and by a factor of 2 if there are two branches for a triple-cut). However, it has a very strong effect on the box integrands in our basis: they must be altered so that each vanishes in all such regions of soft and/or collinear divergence.

Interestingly, the odd box integrands $\mathcal{I}_{A,B,C,D}^o$ in (2.6) already vanish in every collinear region by virtue of the fact that these regions are parity-even. However, the scalar boxes, $\mathcal{I}_{A,B,C,D}^e$ in (2.6) must be modified accordingly. Moreover, this modification will *change* which if any of the inflowing momenta $\{p_A, p_B, p_C, p_D\}$ are massless.

Let us use (lower-case) Greek letters to denote a massless momentum; thus, we'll write ' p_α ' for ' p_A ' if $p_A^2=0$ and similarly for $p_\beta, p_\gamma, p_\delta$. Using this, there are three cases to consider, each with different contact terms added to remove their regions of collinear divergence. The result is a basis of numerators for the boxes given by

$$\widehat{\mathbf{n}}_{A,B,C,D}^e \qquad \qquad \qquad := \mathbf{n}_{A,B,C,D}^e \qquad \qquad \qquad (2.10)$$

$$\widehat{\mathbf{n}}_{\alpha,B,C,D}^e := \frac{1}{2} \left(\llbracket p_\alpha, b, c, C \rrbracket + \llbracket b, c, p_C, p_\alpha \rrbracket + \llbracket p_B, p_C \rrbracket a^2 - \llbracket p_{\alpha B}, p_C \rrbracket b^2 \right), \qquad (2.11)$$

$$\widehat{\mathbf{n}}_{\alpha,\beta,C,D}^e \qquad \qquad := \frac{1}{2} \left(\llbracket p_\alpha, b, c, p_C \rrbracket + \llbracket b, c, p_C, p_\alpha \rrbracket - \llbracket p_{\alpha B}, p_C \rrbracket b^2 \right), \qquad (2.12)$$

$$\widehat{\mathbf{n}}_{\alpha,B,\gamma,D}^e \qquad \qquad := \frac{1}{2} \left(\llbracket p_\alpha, b, c, p_\gamma \rrbracket + \llbracket b, c, p_\gamma, p_\alpha \rrbracket \right). \qquad (2.13)$$

Notice that we have used ' $\widehat{\ }$'s' to disambiguate these numerators from those constructed in (2.6).

By virtue of diagonalization implicit in the prescriptivity condition (1), every even box integrand now automatically vanishes in all soft and/or collinear region of loop-momenta and is therefore IR-finite(!). Where do the divergences of amplitudes now go? The answer is that amplitudes in maximally supersymmetric theories, while vanishing on any contour

taken at infinity, no longer vanish on the contours chosen for the triangle integrals. In particular, amplitudes always have support on the one-mass triangles' contours (the only ones responsible soft *and* collinear IR divergences)—with their leading singularities on these contours being simply the tree amplitude.

Thus, amplitudes in maximally supersymmetric theories would take the form

$$\begin{aligned}
\mathcal{A} &=: \mathcal{A}^{\text{fin}} + \mathcal{A}^{\text{div}}, \quad \text{where} \\
\mathcal{A}^{\text{fin}} &:= \sum_{A,B,C,D} \frac{1}{2} \left(f_{A,B,C,D}^1 + f_{A,B,C,D}^2 \right) \widehat{\mathcal{I}}_{A,B,C,D}^e + \frac{1}{2} \left(f_{A,B,C,D}^1 - f_{A,B,C,D}^2 \right) \widehat{\mathcal{I}}_{A,B,C,D}^o, \quad (2.14) \\
\mathcal{A}^{\text{div}} &:= \sum_{\alpha,\beta,C} \mathcal{A}^{\text{tree}} \widehat{\mathcal{I}}_{\alpha,\beta,C}.
\end{aligned}$$

Notice that this is remarkably similar to the form of the ‘chiral box expansion’ described in [33]; in fact, the only distinction between the basis here and that of [33] is that we have taken the even and odd combinations of chiral numerators.

Chapter 3 | Building a Non-Planar Integrand Basis at Two Loops

To choose particular set of prescriptive integrand basis elements—for any power-counting, for any multiplicity—requires a spanning set of contours. As enumerated in table 1.2 above, the complete, non-planar triangle power-counting basis for six external particles requires that we specify 373 contours of integration. From only these, the integrand basis would be uniquely specified by the prescriptivity requirement (1). However, this is easier said than done.

To help illustrate how this can be done iteratively, with only minimal cleverness (or headache), it is worthwhile to describe how this can be done in stages:

1. For each integrand topology Γ_I ,
 - (a) choose a spanning set of maximal-dimensional contours $\{\Omega_I^i\}$ to define its top-level numerators—each of which encircles all propagators of the given integrand topology.
The number of such numerators must equal the number of **top-level** degrees of freedom in the integrand basis.
n.b. ensure the *set* of contours is invariant under all graph isomorphisms.
 - (b) choose a *spanning set* of *initial* numerators $\{\hat{\mathbf{n}}_I^i\}$ in the chosen integrand basis (with the desired power-counting) which is full-rank on the chosen contours; that is, make sure the *period matrix*

$$\oint_{\Omega_I^i} \mathcal{I}_I^j = \mathbf{M}_{ij} \tag{3.1}$$

is full-rank.

- (c) diagonalize these *initial* numerators to give ‘block-diagonal’ **top-level** numerators $\{\tilde{\mathbf{n}}_I^i\}$; specifically, define

$$\tilde{\mathbf{n}}_I^i := (\mathbf{M}^{-1})_{ji} \hat{\mathbf{n}}_I^j. \quad (3.2)$$

The set of these numerators for each topology are now ‘*block-diagonal*’—meaning that they are diagonal on their defining contours.

2. Diagonalize each numerator against the entire basis.

Provided all propagators of each graph are cut as part of each of its defining contours, then the only contours which need be checked are those which involve subsets of a given graph’s propagators—that is, its daughter topologies (or ‘contact terms’). Because graph inclusion is triangular, diagonalization is analogous to diagonalizing an upper-triangular matrix.

- (a) for each daughter topology $\Gamma_J \prec \Gamma_I$ determine the period integrals

$$\oint_{\Omega_J^j} \tilde{\mathcal{I}}_I^i = (\mathbf{M}_{IJ})_{ij}, \quad (3.3)$$

and *remove* these ‘contact terms’ according to

$$\tilde{\mathcal{I}}_I^i \mapsto \tilde{\mathcal{I}}_I^i - (\mathbf{M}_{IJ})_{ij} \tilde{\mathcal{I}}_J^j. \quad (3.4)$$

Notice that each of these subtractions involves terms *proportional to inverse propagators* appearing in Γ_I ; thus, these subtractions have no effect on the periods of the integrands involving their own defining contours.

Provided this is done iteratively, starting with the graphs with the fewest daughters, this process is guaranteed to result in numerators which are globally diagonal—and hence, a basis which is *prescriptive*.

Of course, once contours have been chosen for all topologies (step 1 above), the resulting basis according to the prescriptivity condition (1) will be unique. However, the process above makes this much more manageable—with the most artful step being the choice of initial numerators.

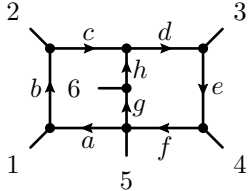
In this section, we'd like to walk the reader through how this was done in the case of \mathfrak{B}_3 for the case of six external particles at two loops.

3.1 Identifying Candidate Numerators and Contours

The starting point in our construction of a basis of two-loop, triangle power-counting integrands in four dimensions is the enumeration of graph topologies and the counting of the number of independent degrees of freedom for which contours must be specified. This data was generated in the recent work [21] and has been summarized in table 1.1 of section 1.2.

For the case of six-particles, varying all the particular distributions of external legs, we find a total of 87 integrand topologies as enumerated in table 1.2. Because each vector space of numerators can be spanned with (sums of) products of generalized inverse propagators, it is straightforward to construct a complete—albeit far from diagonal—initial basis of integrands.

As a representative example, consider a typical non-planar double pentagon, or $\Gamma_{[3,2,3]}$ topology (integrand #11 in our list):



$$\mathfrak{N}_3(\Gamma_{[3,2,3]}) = \text{span} \left\{ [\ell_A]^3 \oplus [\ell_A]^2 [\ell_C] \oplus [\ell_A] [\ell_C]^2 \oplus [\ell_A] [\ell_B] [\ell_C] \right\}. \quad (3.5)$$

Here, $[\ell_A] = [a] = [b] = [c]$, $[\ell_B] = [g] = [h]$, and $[\ell_C] = [d] = [e] = [f]$. As indicated in table 1.2, this vector space of numerators for this topology has 229 total degrees of freedom, of which 8 top-level and the rest (221) are contact terms. A random choice of 8 elements involving inverse-propagators *not* manifestly included in the graph would likely span the space of top-level numerators (and therefore suffice), but would be very far from diagonal in the contours chosen (or in any illuminating form).

Even before discussing the choices for 8 contours required to specify these top-level degrees of freedom, it is worthwhile to build some intuition about what numerators may be *close* to diagonal. Conveniently, for any eight-propagator graph at two loops ($\Gamma_{[4,0,4]}$, $\Gamma_{[4,1,3]}$, $\Gamma_{[4,2,2]}$, $\Gamma_{[3,2,3]}$ in table 1.2—topologies indexed by $I \in \{1, \dots, 12\}$ in our basis), the number of top-level degrees of freedom *exactly* matches the number of solutions to the maximal-cut equations which put all eight propagators on-shell. Thus, there is a one-to-one correspondence between these cut configurations and initial top-level numerators $\tilde{\mathfrak{n}}_{11}^i$ for $i \in \{1, \dots, 8\}$.

To be slightly pedantic, it is worth remembering that our first step is merely to find *initial* ‘block-diagonal’ numerators—which give integrands which satisfy

$$\oint_{\Omega_{11}^j} \tilde{\mathcal{I}}_{11}^i = \delta_{ij}. \quad (3.6)$$

Such integrands are not yet *prescriptive*—as they may have support on the contours involving subsets of propagators (those used to define the top-level degrees of freedom of daughter (‘contact term’) integrand topologies). It is obvious that (3.6) is unchanged by the addition of any such contact terms. And so we still have work to do before we have fully diagonal—prescriptive—integrands.

3.2 Step 1. Guessing a Spanning Set of Top-Level Numerators

As emphasized in section 2, once a spanning set of contours has been chosen, this uniquely fixes every integrand in the basis. This means that in principle the choice of an initial set of spanning numerators for a given topology is unimportant, as the diagonalized numerators are entirely subservient to the contours. In practice, however, carrying out the diagonalization procedure is significantly easier if some thought is given to the initial, pre-diagonal basis of numerators. In particular, the chiral numerators appearing throughout [31, 32] often serve as excellent starting points, even when they require contact term corrections to be rendered diagonal with respect to subtopologies.

There is little subtlety (or mystery) in the construction of ‘nice’ chiral numerators for the eight-propagator integrands in our basis. To illustrate this, let us continue the double-pentagon example of (3.5). In the notation of the ancillary files, this graph is numbered #11, and has the topology shown above:

The diagram shows a graph with 5 vertices labeled 1 through 5. Vertex 1 is at the bottom left, 2 at the top left, 3 at the top right, 4 at the bottom right, and 5 at the bottom center. Propagators are labeled as follows: 'a' is a vertical line from 1 to 5; 'b' is a vertical line from 1 to 2; 'c' is a horizontal line from 2 to a central vertex; 'd' is a horizontal line from that central vertex to 3; 'e' is a vertical line from 3 to 4; 'f' is a horizontal line from 4 to 5; 'g' is a vertical line from 5 to a central vertex; 'h' is a horizontal line from that central vertex to the left. A central vertex is also connected to 2 and 3. The number '6' is placed in the center of the graph. To the left of the graph is the label $\mathcal{I}_{11} \leftrightarrow$ and to the right is the label (3.7).

As mentioned above, the eight solutions to the cut equations correspond to the eight leading singularities associated to this graph. A block-diagonal set of numerators can be systematically constructed by the subspace of $\mathfrak{N}_3(\Gamma_{[3,2,3]})$ *not* spanned by this graph’s

contact terms. In practice, however, it is often easier to guess a representative numerator by considering the kinematic conditions imposed on the on-shell loop momenta for each. For the topology (3.7), the top-level degrees of freedom $\{\tilde{\mathbf{n}}_{11}^i\}$ —which, we stress, are only block-diagonal, and *not* yet diagonal with respect to this topology’s daughter graphs—can be chosen by inspection of the solutions to the cut equations.

For most cases of interest, the particular solutions to the cut equations can be identified by the parity of its three-point vertices—with **blue** for the ‘mhv’ solution (all $\tilde{\lambda}$ ’s proportional) and white for the ‘ $\overline{\text{mhv}}$ ’ solution (all λ ’s proportional). When a vertex has multiplicity >3 , no such parity can be indicated—so black vertices are used in our contour diagrams.

For example, we may identify and number the 8 solutions to the maximal-cut equations for the topology \mathcal{I}_{11} in (3.7) as follows:

These figures represent contours $\{\Omega_{11}^1, \dots, \Omega_{11}^8\}$.

It is easier than it may at first appear to construct a numerator which has support on each of the corresponding contours. For example, to construct a numerator which vanishes on all but the first contour, one need only require that it vanish whenever the vertices have the wrong parity. For example, consider the tentative numerator

$$\tilde{\mathbf{n}}_{11}^1 := \llbracket p_1, b, c, h, g, p_4, e, d \rrbracket ; \quad (3.9)$$

this numerator vanishes whenever $\lambda_1 \propto \lambda_b$ or $\lambda_c \propto \lambda_h$ or when $\lambda_e \propto \lambda_d$ —that is, on all cases where the vertex involving p_1 , p_3 or the top-middle vertex is colored blue, at least one of which is the case for every contour *except* Ω_{11}^1 . (To see this, recall the definition of “ $\llbracket \dots \rrbracket$ ” in (2.7).) Moreover, it is not hard to verify that this numerator gives rise to an

integrand which integrates to 1 on Ω_{11}^1 . That is,

$$\oint_{\Omega_{11}^i} \tilde{\mathcal{I}}_{11}^1 := \oint_{\Omega_{11}^i} d^4 \ell_1 d^4 \ell_2 \frac{\tilde{\mathbf{n}}_{11}^1}{a^2 b^2 c^2 d^2 e^2 f^2 g^2 h^2} = \begin{cases} 1 & i = 1 \\ 0 & i \neq 1 \end{cases}. \quad (3.10)$$

Continuing in this way results in an initial ‘block-diagonal’ set of numerators for topology #11. Specifically, we find that the following numerators are diagonal on the contours for Ω_{11} :

$$\begin{aligned} \tilde{\mathbf{n}}_{11}^1 &:= \llbracket p_1, b, c, h, g, p_4, e, d \rrbracket, & \tilde{\mathbf{n}}_{11}^5 &:= \frac{1}{2} \left(\llbracket e, d, c, b, p_1, g, h, p_4 \rrbracket \right. \\ \tilde{\mathbf{n}}_{11}^2 &:= \frac{1}{2} \left(\llbracket p_1, b, c, h, g, p_3, e, f \rrbracket \right. & & \left. - \llbracket b, c, d, e, p_4, g, h, p_1 \rrbracket \right), \\ & \quad \left. - \llbracket p_4, e, d, h, g, p_2, b, a \rrbracket \right), & \tilde{\mathbf{n}}_{11}^6 &:= - \llbracket p_4, e, d, h, g, p_1, b, c \rrbracket, \\ \tilde{\mathbf{n}}_{11}^3 &:= \llbracket e, d, h, g, a, b, p_2, p_4 \rrbracket, & \tilde{\mathbf{n}}_{11}^7 &:= \frac{1}{2} \left(\llbracket f, p_1, b, c, h, g, p_3, e \rrbracket \right. \\ \tilde{\mathbf{n}}_{11}^4 &:= \frac{1}{2} \left(\llbracket p_4, e, d, c, b, p_1, g, h \rrbracket \right. & & \left. - \llbracket a, p_4, e, d, h, g, p_2, b \rrbracket \right), \\ & \quad \left. - \llbracket p_1, b, c, d, e, p_4, g, h \rrbracket \right), & \tilde{\mathbf{n}}_{11}^8 &:= - \llbracket b, c, h, g, f, e, p_3, p_1 \rrbracket. \end{aligned} \quad (3.11)$$

In cases where these numerators have factors of 2, this reflects contour-graph isomorphisms in (3.8). It is not hard to verify that these numerators are all unit on their corresponding contour, and vanish on all the others. Thus, these numerators provide good starting points for further diagonalization (against daughter-topology contours).

Since all eight-propagator integrands have exactly the same number of solutions to the cut equations as numerator degrees of freedom, this procedure can be repeated without any subtlety whatsoever for every such topology.

There is a single case at six particles, however, where coloring of the vertices alone does not suffice to distinguish all solutions to the maximal cut equations. The exceptional case involves topology #10 in our basis:

$$\mathcal{I}_{10} \leftrightarrow \begin{array}{c} \begin{array}{ccccc} & 2 & & & 3 \\ & \diagdown & & & \diagup \\ & c & & & d \\ \bullet & & \bullet & & \bullet \\ & 6 & & & h \\ & \diagup & & & \diagdown \\ & b & & & e \\ \bullet & & \bullet & & \bullet \\ & 5 & & & g \\ & \diagdown & & & \diagup \\ & a & & & f \\ & \diagup & & & \diagdown \\ 1 & & & & 4 \end{array} \end{array}. \quad (3.12)$$

For two sets of ‘colorings’ of this graph (contours encoded by the parity of the three-point vertices), there are two pairs of solutions to the cut equations related to the choice of sign in front of the square root of $\Delta^2 := \llbracket p_{12}, p_{34} \rrbracket^2 - 4s_{12}s_{34}$. In each case, we may match these two leading singularities with numerators that are chiral, or parity-even and parity-odd; throughout this work, we always choose the latter. Thus, for example, we choose the

following pair of contours:

$$\begin{aligned}
\Omega_{10}^2 := & \begin{array}{c} \begin{array}{ccc} 2 & & 3 \\ \bullet & & \circ \\ \hline 6 & & \\ \hline \circ & & \bullet \\ \hline 5 & & \\ \hline 1 & & 4 \\ \text{(odd)} \end{array} & \leftrightarrow \tilde{\mathbf{n}}_{10}^2 := -\frac{1}{2} \llbracket [e, p_4, p_1, b, c, d] \Delta \rrbracket; \\ & \end{array} \\
\Omega_{10}^4 := & \begin{array}{c} \begin{array}{ccc} 2 & & 3 \\ \bullet & & \circ \\ \hline 6 & & \\ \hline \circ & & \bullet \\ \hline 5 & & \\ \hline 1 & & 4 \\ \text{(even)} \end{array} & \leftrightarrow \tilde{\mathbf{n}}_{10}^4 := \frac{1}{4} \left(\llbracket [g, p_2, b, a, f, e, p_3, h] \rrbracket - \llbracket [p_1, b, c, d, e, p_4, g, h] \rrbracket \right. \\ & \left. + \llbracket [p_4, e, d, c, b, p_1, g, h] \rrbracket - \llbracket [g, p_3, e, f, a, b, p_2, h] \rrbracket \right). \\ & \end{array}
\end{aligned} \tag{3.13}$$

Nota bene: the labels ‘even’ and ‘odd’ do *not* refer to parity: they refer to the *even* or *odd* sum of the multiple solutions to the corresponding contour. In addition to these, there are two more cases which have been split into even/odd combinations; these are related to those of (3.13) by an up/down flip of the graphs.

3.3 Step 2. Block-Diagonalization with Respect to a Choice of Contours

While the contour specification for eight-propagator integrand topologies is quite rigid, for integrands with fewer propagators there is significantly more freedom. By virtue of the requirement that the basis be diagonal in contours, these choices have significant effects on the rest of the basis, including the contact terms of the eight-propagator integrands. A simple one-loop analogue of this freedom is in the normalization of the (scalar) triangle integrand. In sections 2.2.1 and 2.2.2 we emphasized that the form of the triangle power-counting basis, as well as what features were made manifest, depended heavily on whether the (one and two-mass) triangles were normalized at infinite loop momentum or in the soft and/or collinear regions. This phenomenon is even more prominent at two loops, where every integrand topology with fewer than eight propagators requires a choice of contours which has trickle-up (and down) effects on the rest of the basis.

The conventions for our contour choices are as follows. Whenever an integrand topology is such that soft and/or collinear residues are accessible, we choose a corresponding contour as part of our spanning set. When there are no such contours (analogous to the three-mass triangle at one loop) we choose contours involving (at least) one loop-momentum cycle in the graph being sent to infinity. In addition, when the scalar graph

topology has non-trivial graph automorphisms, our contour choices are such that the entire *set* (but not necessarily the individual contours themselves) is invariant up to overall signs. We shall illustrate the rôle of graph symmetries in greater detail below.

The motivation for our preference for soft and/or collinear contours is simple: we aim to construct a basis of integrands maximally stratified according to IR finiteness or divergence. We expect that every integrand *not* normalized on a soft or collinear contour will vanish entirely in every such region of loop momentum space, which is highly suggestive of it being infrared finite upon integration. In the representation of an amplitude, our basis is designed to match the IR-divergence of the amplitude manifestly, while every other integrand with a non-vanishing coefficient vanishing (by construction) in all collinear regions.

3.3.1 Requiring the Set of Contours be Graph Symmetric

The attentive reader may have noted that in the top-level numerators of the non-planar double pentagon example (3.11), several of the numerators had ‘symmetry factors’ in their definition. In this case, it is natural—though not essential—to use numerators which respect the symmetries of the leading singularity graphs associated with the contours. For contours involving composite conditions, wherein at least one set of momenta are either soft and/or collinear, our prescriptive basis of integrands always respects the symmetries of the composite leading singularities. Provided this is done throughout the basis for leading singularities with amplitude support in sYM, any such amplitude integrand’s representation is simple to write down—namely, in the diagonal basis, the integrand will be a sum of inequivalent leading singularities, each decorated by the corresponding basis element [35].

In addition to contours which have amplitude-support in sYM, there are many degrees of freedom in our basis normalized on contours involving infinite loop momenta. In these cases, our convention is to impose a slightly less restrictive symmetry constraint: we require only that the *set* of numerators associated with contours defined at infinity to be closed under the automorphism group of the graph.

To explain our conventions in further detail, let us consider an example in which the automorphism group is non-trivial. Among others, we have a double-box topology #17 with eight degrees of freedom

$$\mathcal{I}_{17} \leftrightarrow \begin{array}{c} 2 \qquad \qquad 3 \\ \swarrow \quad \quad \searrow \\ \xrightarrow{c} \quad \quad \xrightarrow{d} \\ \swarrow \quad \quad \searrow \\ 1 \qquad \qquad 4 \\ \uparrow \quad \quad \downarrow \\ \xleftarrow{a} \quad \quad \xrightarrow{f} \\ \swarrow \quad \quad \searrow \\ 6 \qquad \qquad 5 \\ \uparrow \quad \quad \downarrow \\ \xrightarrow{b} \quad \quad \xrightarrow{e} \\ \swarrow \quad \quad \searrow \\ 1 \qquad \qquad 4 \\ \uparrow \quad \quad \downarrow \\ \xrightarrow{g} \end{array}, \quad (3.14)$$

two contours of which are defined as even combinations of contours taken by starting from a heptacut and sending one loop-momentum cycle to infinity:

$$\Omega_{17}^4 := \left\{ \begin{array}{c} 2 \qquad \qquad 3 \\ \swarrow \quad \quad \searrow \\ \xrightarrow{\quad} \quad \quad \xrightarrow{\quad} \\ \swarrow \quad \quad \searrow \\ 1 \qquad \qquad 4 \\ \uparrow \quad \quad \downarrow \\ \xleftarrow{\quad} \quad \quad \xrightarrow{\quad} \\ \swarrow \quad \quad \searrow \\ 6 \qquad \qquad 5 \\ \uparrow \quad \quad \downarrow \\ \xrightarrow{\quad} \end{array} \right\} + \left\{ \begin{array}{c} 2 \qquad \qquad 3 \\ \swarrow \quad \quad \searrow \\ \xrightarrow{\quad} \quad \quad \xrightarrow{\quad} \\ \swarrow \quad \quad \searrow \\ 1 \qquad \qquad 4 \\ \uparrow \quad \quad \downarrow \\ \xleftarrow{\quad} \quad \quad \xrightarrow{\quad} \\ \swarrow \quad \quad \searrow \\ 6 \qquad \qquad 5 \\ \uparrow \quad \quad \downarrow \\ \xrightarrow{\quad} \end{array} \right\} \leftrightarrow \tilde{\mathbf{n}}_{17}^4 := \frac{1}{2} [[c, d, e, p_4, p_1, b]], \quad (3.15)$$

$$\Omega_{17}^8 := \left\{ \begin{array}{c} 2 \qquad \qquad 3 \\ \swarrow \quad \quad \searrow \\ \xrightarrow{\quad} \quad \quad \xrightarrow{\quad} \\ \swarrow \quad \quad \searrow \\ 1 \qquad \qquad 4 \\ \uparrow \quad \quad \downarrow \\ \xleftarrow{\quad} \quad \quad \xrightarrow{\quad} \\ \swarrow \quad \quad \searrow \\ 6 \qquad \qquad 5 \\ \uparrow \quad \quad \downarrow \\ \xrightarrow{\quad} \end{array} \right\} + \left\{ \begin{array}{c} 2 \qquad \qquad 3 \\ \swarrow \quad \quad \searrow \\ \xrightarrow{\quad} \quad \quad \xrightarrow{\quad} \\ \swarrow \quad \quad \searrow \\ 1 \qquad \qquad 4 \\ \uparrow \quad \quad \downarrow \\ \xleftarrow{\quad} \quad \quad \xrightarrow{\quad} \\ \swarrow \quad \quad \searrow \\ 6 \qquad \qquad 5 \\ \uparrow \quad \quad \downarrow \\ \xrightarrow{\quad} \end{array} \right\} \leftrightarrow \tilde{\mathbf{n}}_{17}^8 := \frac{1}{2} [[b, c, d, e, p_4, p_1]]. \quad (3.16)$$

In addition to these, there are four degrees of freedom normalized on soft contours associated with either the momentum through edges b or e to zero. These contours—and corresponding numerators which are unit on them—are easy to identify:

$$\Omega_{17}^1 := \begin{array}{c} 2 \qquad \qquad 3 \\ \swarrow \quad \quad \searrow \\ \xrightarrow{\quad} \quad \quad \xrightarrow{\quad} \\ \swarrow \quad \quad \searrow \\ 1 \qquad \qquad 4 \\ \uparrow \quad \quad \downarrow \\ \xleftarrow{\quad} \quad \quad \xrightarrow{\quad} \\ \swarrow \quad \quad \searrow \\ 6 \qquad \qquad 5 \\ \uparrow \quad \quad \downarrow \\ \xrightarrow{\quad} \end{array} \leftrightarrow \tilde{\mathbf{n}}_{17}^1 := s_{12} [[e, d, c, p_4]] + \frac{1}{2} [[b, c, d, e, p_4, p_1]], \quad (3.17)$$

$$\Omega_{17}^5 := \begin{array}{c} 2 \qquad \qquad 3 \\ \swarrow \quad \quad \searrow \\ \xrightarrow{\quad} \quad \quad \xrightarrow{\quad} \\ \swarrow \quad \quad \searrow \\ 1 \qquad \qquad 4 \\ \uparrow \quad \quad \downarrow \\ \xleftarrow{\quad} \quad \quad \xrightarrow{\quad} \\ \swarrow \quad \quad \searrow \\ 6 \qquad \qquad 5 \\ \uparrow \quad \quad \downarrow \\ \xrightarrow{\quad} \end{array} \leftrightarrow \tilde{\mathbf{n}}_{17}^5 := s_{12} [[d, c, p_4, e]] + \frac{1}{2} [[c, d, e, p_4, p_1, b]], \quad (3.18)$$

$$\Omega_{17}^3 := \begin{array}{c} 2 \qquad \qquad 3 \\ \swarrow \quad \quad \searrow \\ \xrightarrow{\quad} \quad \quad \xrightarrow{\quad} \\ \swarrow \quad \quad \searrow \\ 1 \qquad \qquad 4 \\ \uparrow \quad \quad \downarrow \\ \xleftarrow{\quad} \quad \quad \xrightarrow{\quad} \\ \swarrow \quad \quad \searrow \\ 6 \qquad \qquad 5 \\ \uparrow \quad \quad \downarrow \\ \xrightarrow{\quad} \end{array} \leftrightarrow \tilde{\mathbf{n}}_{17}^3 := s_{34} [[c, d, p_1, b]] - \frac{1}{2} [[d, c, b, p_1, p_4, e]], \quad (3.19)$$

$$\Omega_{17}^7 := \leftrightarrow \tilde{\mathbf{n}}_{17}^7 := s_{34} [[b, c, d, p_1]] - \frac{1}{2} [[e, d, c, b, p_1, p_4]]. \quad (3.20)$$

The appearance of the colored numerators in the expressions (3.17) are needed in order for the combined numerators to vanish on the defining contours in (3.15). The rest of the eight-dimensional basis of numerators is furnished by contours defined by starting from a hepta-cut and imposing collinearity at the vertex involving edges $\{c, d, g\}$,

$$\Omega_{17}^2 := \leftrightarrow \tilde{\mathbf{n}}_{17}^2 := - [[e, d, a, b, p_2, p_4]], \quad (3.21)$$

$$\Omega_{17}^6 := \leftrightarrow \tilde{\mathbf{n}}_{17}^6 := - [[p_4, e, d, a, b, p_2]]. \quad (3.22)$$

$$(3.23)$$

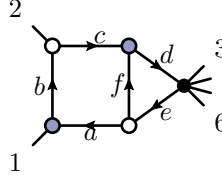
3.3.2 Contours Involving Double-Poles

There is one additional complication regarding contour choices: for triangle power-counting, there are an *insufficient* number of maximal co-dimension residues of logarithmic type to fill out the basis. Said differently, the basis of integrands cannot be spanned by polylogarithmic integrals of uniform and *maximal* transcendental weight. Instead, there are some degrees of freedom must be normalized on contours involving double-poles. This phenomenon first appears at the six-propagator level, and is exemplified by considering the following example, #47 in our basis:

$$\mathcal{I}_{47} \leftrightarrow \quad (3.24)$$

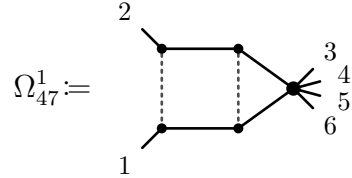
For triangle power-counting, this topology requires a choice of three contours. However, in this case, due to the degenerate kinematics where only a single vertex is massive, there

is only a single independent contour which is logarithmic. We can detect the presence of double-poles in this topology's cut structure by considering a hexa-cut where all six propagators are on-shell. One solution to the cut equations may be parametrized in a basis of spinors $\{\lambda_1, \tilde{\lambda}_1, \lambda_2, \tilde{\lambda}_2\}$ as,

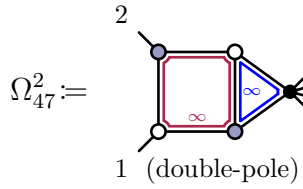


$$\leftrightarrow b^* = \alpha \lambda_2 \tilde{\lambda}_1, \quad d^* = [\beta \lambda_1 + \alpha(1 - \beta) \lambda_2] \left(\tilde{\lambda}_1 + \frac{1}{\alpha} \tilde{\lambda}_2 \right), \quad (3.25)$$

where the Jacobian of the hexa-cut is $J = s_{12}^2 \alpha \beta$. Trivially, we see that the scalar numerator $\tilde{\mathbf{n}}_{47}^1 = s_{12}^2$ yields a logarithmic two-form $d \log \alpha d \log \beta$, and the corresponding contour may be normalized at some combination of $\alpha, \beta \rightarrow \{0, \infty\}$. However, it is also easy to see that there is no other independent contour (accessible using a loop-momentum dependent numerator) which does not involve a double-pole (at infinity) in either α or β . Indeed, to span the full space of triangle power-counting numerators for this topology, we are forced to introduce two double-pole numerators $\tilde{\mathbf{n}}_{47}^{2,3}$. Since the power-counting allows an ℓ_1 -dependent numerator, we see that any integrand proportional to α on the cut (3.25) will have a double-pole in the (ordered) limit $\beta, \alpha \rightarrow \infty$; these two conditions, together with the hexacut, define the double-pole contour. The parity conjugate of this contour fills out the rest of the basis, and a block-diagonal set of numerators is:

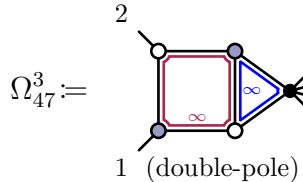


$$\Omega_{47}^1 := \quad \leftrightarrow \tilde{\mathbf{n}}_{47}^1 := s_{12} \llbracket c, p_{12} \rrbracket, \quad (3.26)$$



$$\Omega_{47}^2 := \quad \leftrightarrow \tilde{\mathbf{n}}_{47}^2 := \frac{1}{2} (\llbracket a, p_1, p_2, p_{45} \rrbracket + \llbracket p_2, p_1, p_{45}, c \rrbracket), \quad (3.27)$$

1 (double-pole)



$$\Omega_{47}^3 := \quad \leftrightarrow \tilde{\mathbf{n}}_{47}^3 := \frac{1}{2} (\llbracket c, p_2, p_1, p_{45} \rrbracket + \llbracket p_1, p_2, p_{45}, a \rrbracket). \quad (3.28)$$

1 (double-pole)

While the appearance of double-pole degrees of freedom may seem avoidable in the previous example, at the five propagator level there are, in fact, topologies where there exists *no* logarithmic contours whatsoever. An example of this is #85 in our basis, the

$\Gamma_{[2,1,2]}$ topology:

$$\mathcal{I}_{85} \leftrightarrow \begin{array}{c} \begin{array}{c} 2 \\ \diagup \quad \diagdown \\ \bullet \quad \bullet \\ \diagdown \quad \diagup \\ 1 \end{array} \quad \begin{array}{c} b \\ \rightarrow \\ e \\ \leftarrow \\ d \end{array} \quad \begin{array}{c} 3 \\ \diagdown \quad \diagup \\ \bullet \quad \bullet \\ \diagup \quad \diagdown \\ 4 \\ 5 \\ 6 \end{array} \end{array} \quad (3.29)$$

The only allowed numerator for triangle power-counting is a scalar and—regardless of its normalization—the resulting integrand has double-poles in its cut structure (indicative of a drop in transcendental weight upon integration). In particular, a contour defined by imposing collinearity at both three-point vertices in (3.29) and sending the loop momenta to infinity may be accessed by starting from the co-dimension six configuration

$$a = d = (\alpha\lambda_1 + \beta\lambda_2) \left[\tilde{\lambda}_1 - \left(\frac{\alpha+1}{\beta} \right) \tilde{\lambda}_2 \right], \quad J = -s_{12}\beta. \quad (3.30)$$

Upon taking a residue at $\beta \rightarrow \infty$, the integrand with scalar numerator s_{12} evaluates on (3.30) to

$$\underset{(3.30)}{\text{Res}} \left(\mathcal{I}_{85}^1 \right) = \frac{-d\alpha d\beta}{\beta}. \quad (3.31)$$

After taking an additional residue at $\beta \rightarrow \infty$, we may choose to normalize this degree of freedom to be 1 at the double-pole at $\alpha \rightarrow \infty$. In fact, however, this contour prescription does not enjoy the up-down flip symmetry of the scalar graph in (3.29). Using a contour which is compatible with the symmetries of the scalar graph produces a symmetry factor in the corresponding numerator, which is $\mathbf{n}_{85}^1 := \frac{1}{2}s_{12}$. (Note that this is indeed the globally diagonal numerator because this integrand has no contact terms whatsoever, which explains why we have omitted the \sim label above \mathbf{n}_{85}^1 .) Diagrammatically, we indicate this contour as:

$$\Omega_{85}^1 := \begin{array}{c} \begin{array}{c} 2 \\ \diagup \quad \diagdown \\ \bullet \quad \bullet \\ \diagdown \quad \diagup \\ 1 \end{array} \quad \begin{array}{c} \infty \\ \leftarrow \\ \infty \\ \rightarrow \end{array} \quad \begin{array}{c} 3 \\ \diagdown \quad \diagup \\ \bullet \quad \bullet \\ \diagup \quad \diagdown \\ 4 \\ 5 \\ 6 \end{array} \end{array} \quad (3.32)$$

(odd) double-pole

3.4 Step 3. Global Diagonalization of the Basis

The numerators obtained as described in the previous section 3.2 are locally-diagonal, and provide an excellent starting point in the construction of a complete, globally-diagonal basis. If we denote the set of block-diagonal integrands for topology I as $\{\tilde{\mathcal{I}}_I^i\}$ and the corresponding contours as $\{\Omega_I^i\}$, where i is an index running over the number of

top-level degrees of freedom in triangle power-counting basis for the I th topology, then by construction we have

$$\oint_{\Omega_I^j} \tilde{\mathcal{I}}_I^i = \delta_{i,j}. \quad (3.33)$$

However, generically the integrands of the parent topologies will still have support on the contours of their daughters (the set of graphs generated by contracting some number of internal edges). That is, the complete top-level and contact term period matrix is of the form

$$\oint_{\Omega_J^j} \tilde{\mathcal{I}}_I^i = \begin{cases} \delta_{ij} & I = J, \\ (\mathbf{M}_{IJ})_{ij} & I \neq J. \end{cases} \quad (3.34)$$

By contrast, in a globally diagonal basis the contact-term matrices (\mathbf{M}_{IJ}) *must* vanish identically for all pairs I, J .

Notice that the set of period matrices \mathbf{M}_{IJ} above is automatically *upper-triangular* in its indices $\{I, J\}$: it is a consequence of the triangular-nature of graph inclusion: \mathbf{M}_{IJ} vanishes for any graph $\Gamma_J \not\prec \Gamma_I$ —that is for any set of contours $\{\Omega_J\}$ *not* corresponding to a daughter of the graph Γ_I . This makes it extremely easy to diagonalize the entire matrix.

To diagonalize the partially-diagonal basis (3.34), it is useful to take a ‘bottom-up’ approach. To begin, we partition the 87 integrand topologies relevant for two-loop, triangle power-counting at six particles according to the number of propagators. Thus, at the ‘bottom’ of the list are the five-propagator, $\Gamma_{[2,1,2]}$ topologies, each with a single degree of freedom. Trivially, these basis elements already vanish on every other defining contour by virtue of the fact that they lack the additional propagators necessary to access the six-propagator and higher contours. That is, in a slight abuse of notation we have schematically

$$\oint_{\Omega_{6,7, \text{ or } 8 \text{ props}}} \mathcal{I}_{[2,1,2]} = 0, \quad (3.35)$$

where $\Omega_{6,7, \text{ or } 8 \text{ props}}$ denotes any six-, seven- or eight-propagator-cutting contour, and $\mathcal{I}_{[2,1,2]}$ any five-propagator integrand in the basis.

The next step is to diagonalize each of the six-propagator integrands, which are of either $\Gamma_{[3,0,3]}$, $\Gamma_{[2,2,2]}$ or $\Gamma_{[3,1,2]}$ type, with respect to every five-propagator graph obtained by single internal edge contractions. Let us illustrate how this works in practice with a particular example: in the notation of the ancillary files of this paper, one of the degrees

of freedom of topology #61,

$$\mathcal{I}_{61} \leftrightarrow 1 \text{ --- } \begin{array}{c} \text{---} b \text{---} \\ \text{---} f \text{---} \\ \text{---} c \text{---} \\ \text{---} a \text{---} \\ \text{---} e \text{---} \\ \text{---} d \text{---} \end{array} \begin{array}{l} 2 \\ 3 \\ 4 \\ 5 \end{array} , \quad (3.36)$$

is naturally associated with a contour where edges $a, f \rightarrow 0$ are soft. A corresponding numerator which is unit on this contour (and which is already diagonal with respect to the other five top-level contours of this topology) is,

$$1 \text{ --- } \begin{array}{c} \text{---} \\ \text{---} \\ \text{---} \\ \text{---} \\ \text{---} \\ \text{---} \end{array} \begin{array}{l} 2 \\ 3 \\ 4 \\ 5 \end{array} \leftrightarrow \tilde{\mathbf{n}}_{61}^1 = [[c, d, p_1, p_6]]. \quad (3.37)$$

The six contact-term degrees of freedom of this integrand are proportional to the inverse propagators of the graph; thus, the final, diagonalized numerator \mathbf{n}_{61}^1 will take the form

$$\mathbf{n}_{61}^1 := \tilde{\mathbf{n}}_{61}^1 + c_1 a^2 + \dots + c_6 f^2. \quad (3.38)$$

Consider the term proportional to e^2 . Upon collapsing this edge in (3.36), we obtain (a re-labelled version of) the five-propagator topology #78,

$$\mathcal{I}_{78} \leftrightarrow 1 \text{ --- } \begin{array}{c} \text{---} b \text{---} \\ \text{---} c \text{---} \\ \text{---} a \text{---} \\ \text{---} d \text{---} \\ \text{---} e \text{---} \end{array} \begin{array}{l} 2 \\ 3 \\ 4 \\ 5 \\ 6 \end{array} , \quad (3.39)$$

whose scalar degree of freedom is normalized on the contour

$$\Omega_{78}^1 := 1 \text{ --- } \begin{array}{c} \text{---} \\ \text{---} \\ \text{---} \\ \text{---} \\ \text{---} \\ \text{---} \end{array} \begin{array}{l} 2 \\ 3 \\ 4 \\ 5 \\ 6 \\ \text{(odd)} \end{array} \leftrightarrow \mathbf{n}_{78}^1 := -\frac{1}{2} s_{16}. \quad (3.40)$$

While this contour is an odd combination of two residues, the top-level numerator (3.37) happens to have support on only one of them. An analytic representation of the relevant part of this contour is given by parametrizing $b=0$ and $c=(\lambda_1 + \alpha \lambda_6) \tilde{\lambda}_1$ with Jacobian $J = \alpha s_{16}$, and where the final residue is taken at $\alpha \rightarrow \infty$. The residue of the pre-diagonal integrand #61, degree of freedom $i=1$ may be computed by evaluating the numerator

and dividing by both the Jacobian and the uncut propagator, and we find

$$\oint_{\Omega_{78}^1} \tilde{\mathcal{I}}_{61}^1 = \text{Res}_{\alpha \rightarrow \infty} \left(\frac{[[c, d, p_1, p_6]] d\alpha}{J(d-a)^2} \right) = \text{Res}_{\alpha \rightarrow \infty} \left(\frac{d\alpha}{\alpha} \right) = -1. \quad (3.41)$$

To remove the integrand's support on this contour fixes the contact term involving e^2 to have the coefficient $c_5 = 2\mathbf{n}_{78}^1 := -s_{16}$. Similar calculations for the remaining five contact terms of integrand #61 lead to the final expression for the diagonalized numerator,

$$\mathbf{n}_{61}^1 := [[c, d, p_1, p_6]] - \frac{s_{16}}{2} [c^2 + d^2 + 2(b^2 + e^2)]. \quad (3.42)$$

This procedure must be repeated for every degree of freedom and every topology with six propagators. Once this is done, the resulting basis is diagonal and fully fixed at both the five- and six-propagator levels, and we have

$$\oint_{\Omega_{[2,1,2]}} \mathcal{I}_\gamma = 0, \quad (3.43)$$

where $\gamma \in \{[3, 0, 3], [2, 2, 2], [3, 1, 2]\}$ and $\Omega_{[2,1,2]}$ denotes any five-cut contour.

This same procedure must be iteratively repeated to fix the contact terms of the seven-propagator integrands by demanding orthogonality with respect to both the five- and six-propagator basis elements. For example, the 45 contact term degrees of freedom for topology #38 are fixed by enumerating the daughter topologies (and counting with the appropriate multiplicity)

(3.44)

A final, prescriptive and globally-diagonal basis is obtained by removing all relevant contact terms from the eight-propagator integrands.

The end result of the above procedure is a fully diagonal basis of integrands and contours $\{\mathcal{I}_I^i, \Omega_I^i\}$,

$$\oint_{\Omega_J^j} \mathcal{I}_I^i = \begin{cases} \delta_{ij} & I = J, \\ 0 & I \neq J. \end{cases} \quad (3.45)$$

3.5 Features of the Resulting Basis of Integrands

The triangle power-counting basis of local integrands constructed according to the procedure of section 3 has several noteworthy properties worth emphasizing. First, this basis is prescriptive: every integrand is normalized to be unit on a single co-dimension eight contour, and vanishes on every other contour in the spanning set. Producing a unique representation of an amplitude integrand \mathcal{A} which is of box or triangle power-counting amounts to computing a set of contour integrals

$$\mathcal{A} = \sum_{I,i} \mathbf{a}_I^i \mathcal{I}^i, \quad \text{where} \quad \mathbf{a}_I^i := \oint_{\Omega_I^i} \mathcal{A}. \quad (3.46)$$

The non-zero coefficients \mathbf{a}_I^i are the non-vanishing leading singularities of the amplitude in question. To be clear, this procedure does not require computing *every* leading singularity of an amplitude, but only those in the spanning set of contours $\{\Omega_I^i\}$; all other contours are matched automatically in (3.46) by the completeness of the basis. Furthermore, for all contours not manifestly matched in (3.46), each integrand $\{\mathcal{I}^i\}$ which is *not* normalized on a double-pole at infinity evaluates to either ± 1 or $\pm \frac{1}{2}$. Our basis therefore splits into pure, unit-leading-singularity polylogarithmic integrals as well as integrals which have simple transcendental weight drops upon integration. As amplitude integrands in sYM are free of double-poles, we expect the representation (3.46) is entirely free of transcendental weight drops.

Our basis is also partitioned according to infrared structure. From the complete list of contours (which can be found in the ancillary files), every integrand normalized on a contour in the collinear region of loop momentum space may be identified; these integrands generate infrared divergences upon integration, while every other basis element are explicitly infrared finite. The partitioning according to IR finiteness/divergence will obviously descend to the expression for amplitude integrands (3.46), where every soft-collinear divergence of the amplitude is matched manifestly by individual elements of basis designed to have support on the corresponding soft-collinear contours.

The final basis includes 183 IR-finite integrands and 190 IR-divergent integrands; and of these only 24 have support on double-poles—which should be the only integrands with less than maximal weight.

Chapter 4 | Six-Particle N^k MHV Amplitudes at Two-Loops

As the basis constructed in ref. [119] is complete, it should contain both MHV and NMHV six-particle amplitude integrands. Although the MHV amplitude has been known for some time (given both in [31] and as a special case of [32]), our current basis is distinct; and thus the presentation given here represents a novel cross check on those results. Moreover, representing both the MHV *and* the NMHV amplitude in the *same* basis of master integrands may facilitate the computation of IR-finite quantities such as a non-planar analogue of the ratio function.

For either the MHV or the NMHV amplitude, the leading singularities correspond to color-dressed on-shell functions which are fully Bose-symmetric in the legs entering each vertex tree-amplitude. Each vertex amplitude can be decomposed into color- times kinematic-factors with precise ordering of external according to DDM [120]. Graphically, we can denote this decomposition by the following: for any subset of two legs labelled $\{\alpha, \beta\}$, of each vertex amplitude of an on-shell diagram, we write

$$\begin{array}{c} A \\ \bullet \\ \alpha \quad \beta \end{array} = \sum_{\vec{a} \in \mathfrak{S}(A)} \begin{array}{c} \vec{a} \\ \bullet \\ \alpha \quad \beta \end{array} \times \begin{array}{c} \vec{a} \\ \bullet \\ \alpha \quad \beta \end{array}, \quad (4.1)$$

where the sum is over all $(n-2)!$ permutations $\vec{a} = (a_1, \dots, a_{n-1})$ of the *unordered* set $A := [n] \setminus \{\alpha, \beta\}$ and with color-factors defined as

$$\begin{aligned} f_{\alpha\beta}^{\vec{a}} &:= \sum_{e_i} f^{\alpha a_1 e_1} f^{e_1 a_2 e_2} \dots f^{e_{n-1} a_{n-1} \beta} \\ &=: \begin{array}{c} a_1 \quad a_2 \quad \dots \quad a_{n-1} \\ | \quad | \quad \dots \quad | \\ \alpha \quad e_1 \quad \dots \quad e_{n-1} \quad \beta \end{array} =: \begin{array}{c} \vec{a} \\ \bullet \\ \alpha \quad \beta \end{array}, \quad (4.2) \end{aligned}$$

with f^{abc} being the structure constants of the relevant gauge group. Applying this expansion at every vertex of a two-loop leading singularity results in an expansion in terms of kinematic-dependent on-shell functions built with amplitudes involving *locally ordered* legs times general color-factors of the form

$$\begin{aligned}
 f[\vec{a}, \vec{b}, \vec{c}] &:= \text{diagram} \\
 &= \sum_{e_i} f^{e_1 e_3 e_6} f_{e_1 e_2}^{\vec{a}} f_{e_3 e_4}^{\vec{c}} f_{e_5 e_6}^{\vec{b}} f^{e_2 e_5 e_4}.
 \end{aligned}
 \tag{4.3}$$

This is similar to the decomposition described in [121]. For examples of how this works for color-dressed leading singularities in sYM, see e.g. [31, 32].

4.1 Summing Terms for Amplitudes

The basis of integrands constructed in [119] involved 87 integrand *topologies* corresponding to specific Feynman-propagator graphs which encode their loop-dependent denominators; each of these topologies was then provided with a collection of specific triangle power-counting, loop-dependent numerators—the number of which is determined by the integrand’s propagator-graph according to [21]; their precise form of these numerators was determined by the requirement of prescriptivity (1) with respect to a corresponding choice of contours.

We may denote the integrand with the i th topology ($i \in \{1, \dots, 87\}$) and the j th loop-dependent numerator by $\mathcal{I}_i^j := \mathcal{I}_i \mathbf{n}_i^j$, where \mathcal{I}_i consists of all loop-dependent denominators corresponding to some Feynman graph and \mathbf{n}_i^j denotes a particular, loop-dependent numerator for this integrand topology. In all, the basis described in [119] consists of 373 integrands, each written with a particular choice of external momenta flowing into the graph.

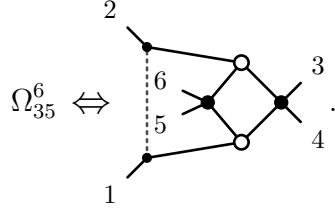
Consider for example the integrand topology numbered 35, with denominator encoded by the Feynman propagators given by

$$\mathcal{I}_{35} \Leftrightarrow \text{diagram}
 \tag{4.4}$$

For this integrand, there are 10 distinct loop-dependent numerators \mathfrak{n}_{35}^j . For example, the 6th such numerator is defined to be [119]

$$\mathfrak{n}_{35}^6 := -s_{12} \left([[a, e, d, c]] - a^2 d^2 + c^2 e^2 \right), \quad (4.5)$$

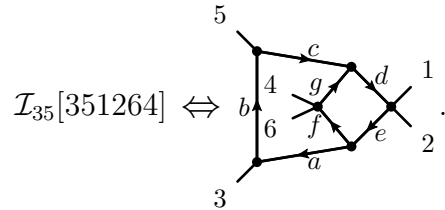
in terms of the bracket $[[\dots]] := \text{tr}_+(\dots)$ and momenta flowing through the various edges of the graph (4.4). This numerator has been fixed by the requirement that $\oint_{\Omega_{35}^6} \mathcal{I}_{35}^6 = 1$, where the contour Ω_{35}^6 can be represented according to



$$\Omega_{35}^6 \Leftrightarrow \text{graph} \quad (4.6)$$

In (4.6), the particular choice of contour is encoded graphically as described in [119]—to which we refer the reader for complete details. (The apparent ‘contact-terms’ appearing in (4.5) are fixed by prescriptivity (1).)

The reader will notice that a particular choice of external legs have been used to encode the *representative* basis integrand \mathcal{I}_i^j . Naturally, permutations of the external legs must be included as well in the summation (2). We may use ‘ $\mathcal{I}_i^j[\sigma]$ ’ to denote the integrand with topology \mathcal{I}_i and numerator \mathfrak{n}_i^j for which the external legs have been relabelled *relative to the reference* integrand according to $[1, \dots, 6] \mapsto [\sigma(1), \dots, \sigma(6)]$ for any permutation $\sigma \in \mathfrak{S}_6$. We may use similar notation $\Omega_i^j[\sigma]$ to denote contours involving permuted leg labels relative to the seeds defined in [119] and $\mathfrak{a}_i^j[\sigma]$ for leading singularities. For example,



$$\mathcal{I}_{35}[351264] \Leftrightarrow \text{graph} \quad (4.7)$$

Clearly, not all relabelings are inequivalent. For example, the integrand \mathcal{I}_{35}^6 has only $45 = 6!/(2^4)$ inequivalent permutations of the external legs, as permuting the pairs of legs $(3 \leftrightarrow 4)$ or $(5 \leftrightarrow 6)$; and swapping the sets $(3, 4) \leftrightarrow (5, 6)$ or flipping the graph vertically each leave the integrand invariant after relabeling the (arbitrary) edge labels.

In general, the number of inequivalent relabelings of a given integrand depends not only on the integrand topology (which may have nontrivial graph automorphisms), but also on the symmetries of its numerator—or, equivalently, the symmetries enjoyed by

its defining contour of integration. Letting $\mathfrak{S}_i^j \subset \mathfrak{S}_6$ denote the subset of inequivalent relabelings of the external legs, the complete form of the summand in (2) can be written as

$$\mathcal{A} = \sum_{i,j} \sum_{\sigma \in \mathfrak{S}_i^j} \mathfrak{a}_i^j[\sigma] \mathcal{I}_i^j[\sigma]. \quad (4.8)$$

Actually, there is one final subtlety to mention. Although for any given distribution of external legs $\mathcal{I}_i^j[\sigma]$ encodes a distinct integrand for each j , it may be that the j th contour/integrand for one permutation of legs corresponds to the $k \neq j$ th integrand/contour for a different permutation of legs. For example, consider two of the eight contours defining the integrands \mathcal{I}_{10}^j :

$$\begin{array}{cc} \Omega_{10}^4[123456] & \Omega_{10}^7[123456] \\ \text{(even)} & \text{(even)} \end{array} \quad (4.9)$$

It is easy to see that $\Omega_{10}^4[214356] \simeq \Omega_{10}^7[123456]$; as such, including both terms in the summand (4.8) would double-count such contributions. For all cases where this occurs, we choose to sum over all the leg-permuted images of only *one* choice of the relevant seeds.

Among the 373 contours used to define the basis given in [119], a large fraction of these have manifestly no support for amplitudes in sYM. Specifically, the basis contours include 96 involving poles at infinity, 23 involving double-poles (associated with transcendental weight-drops), and 137 which have support on collinear *but not soft* regions of loop momenta; all these integrands have vanishing leading singularities. In all, there are only 139 (of the 373) contours which define the basis that have support for amplitudes of some N^k MHV-degree.

As most of the contours defining the integrand basis do not have support of amplitudes, relatively few are required to express each N^k MHV amplitude. In particular, we find that the MHV (or $\overline{\text{MHV}} \simeq N^2$ MHV) amplitude requires only 38 permutation-seeds, and the NMHV amplitude requires only 80. Summing over all relevant relabelings of external legs, these amplitudes involve a total of 7,680 and 21,135 terms, respectively.

4.2 The Six-Particle MHV Amplitude

The relevant on-shell functions for MHV amplitudes (at any loop order or multiplicity) were classified in [17] and can be represented at two loops concretely in terms of a function

$$\Gamma[(a_1, \dots, a_{-1}), (b_1, \dots, b_{-1}), (c_1, \dots, c_{-1})] \quad (4.10)$$

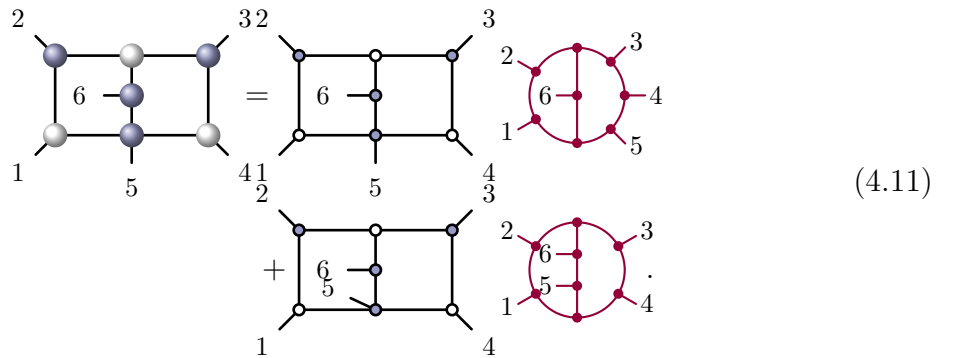
defined in [31, 32] (see also [45]). This function is invariant under permutations of the ordering of its arguments and under cyclic rotations of each argument separately.

All non-vanishing leading singularities of the six particle MHV amplitude were given in [31]; these correspond to 38 particular contours for (3). As these 38 contours were among those used in the prescriptive basis of ref. [119], each of these coefficients will be the same (while the integrands are rather different). Beyond permuting the leg-labels for the permutation-seeds of each basis integrand of ref. [119] (used here) relative to those used in ref. [31], these coefficients are identical.

4.3 The Six-Particle NMHV Amplitude

For the six-particle NMHV amplitude, the kinematic part of all leading singularities (for arbitrary loop-order) were classified in ref. [122]. For each of the defining contours of the basis \mathfrak{B}_3 , identifying the correct kinematic superfunction from among those classified in [122] was done by explicit calculation—by computing the products of on-shell (locally cyclically-ordered, tree-)amplitudes evaluated on the corresponding maximal-cut in loop-integrand space, and summing over all the states that could be exchanged between them.

For example, consider the following color-dressed on-shell function for NMHV—which would appear as the coefficient of \mathcal{I}_{11}^1 in the basis of [119]:



$$\begin{array}{c} \begin{array}{ccc} \begin{array}{c} 2 \\ \bullet \\ \diagup \quad \diagdown \\ \bullet \quad \bullet \\ \diagdown \quad \diagup \\ \bullet \\ 1 \end{array} & \begin{array}{c} 32 \\ \bullet \\ \diagup \quad \diagdown \\ \bullet \quad \bullet \\ \diagdown \quad \diagup \\ \bullet \\ 5 \end{array} & \begin{array}{c} 3 \\ \bullet \\ \diagup \quad \diagdown \\ \bullet \quad \bullet \\ \diagdown \quad \diagup \\ \bullet \\ 4 \end{array} \\ \text{6} & \text{6} & \text{6} \\ \text{5} & \text{5} & \text{5} \end{array} \\ = & \begin{array}{ccc} \begin{array}{c} 41 \\ 2 \\ \bullet \\ \diagup \quad \diagdown \\ \bullet \quad \bullet \\ \diagdown \quad \diagup \\ \bullet \\ 1 \end{array} & \begin{array}{c} 5 \\ \bullet \\ \diagup \quad \diagdown \\ \bullet \quad \bullet \\ \diagdown \quad \diagup \\ \bullet \\ 4 \end{array} & \begin{array}{c} 4 \\ 3 \\ \bullet \\ \diagup \quad \diagdown \\ \bullet \quad \bullet \\ \diagdown \quad \diagup \\ \bullet \\ 1 \end{array} \\ \text{6} & \text{6} & \text{6} \\ \text{5} & \text{5} & \text{5} \end{array} \\ + & \begin{array}{ccc} \begin{array}{c} 4 \\ 3 \\ \bullet \\ \diagup \quad \diagdown \\ \bullet \quad \bullet \\ \diagdown \quad \diagup \\ \bullet \\ 1 \end{array} & \begin{array}{c} 5 \\ \bullet \\ \diagup \quad \diagdown \\ \bullet \quad \bullet \\ \diagdown \quad \diagup \\ \bullet \\ 4 \end{array} & \begin{array}{c} 4 \\ 3 \\ \bullet \\ \diagup \quad \diagdown \\ \bullet \quad \bullet \\ \diagdown \quad \diagup \\ \bullet \\ 1 \end{array} \\ \text{6} & \text{6} & \text{6} \\ \text{5} & \text{5} & \text{5} \end{array} \end{array} \quad (4.11)$$

Comparing against the reference formulae in ref. [122], we may identify the relevant kinematic factors as being identified with the functions

$$\begin{array}{cc}
 \begin{array}{c} 2 \quad 3 \\ \diagdown \quad \diagup \\ \text{---} \text{---} \text{---} \\ \diagup \quad \diagdown \\ 1 \quad 4 \\ \text{---} \text{---} \text{---} \\ \diagdown \quad \diagup \\ 5 \quad 6 \end{array} & \begin{array}{c} 2 \quad 3 \\ \diagdown \quad \diagup \\ \text{---} \text{---} \text{---} \\ \diagup \quad \diagdown \\ 1 \quad 4 \\ \text{---} \text{---} \text{---} \\ \diagdown \quad \diagup \\ 5 \quad 6 \end{array} \\
 = -f_2^c[263451] & = -f_5[145632]
 \end{array} \tag{4.12}$$

We refer the reader to [122] for details on the definitions of these superfunctions.

In all, we find 80 non-vanishing leading singularities for the contours $\{\Omega_i\}$ defining the basis in [119]. Interestingly, of the 10 classes of leading singularities enumerated in [122], the only ones that appear at two loops are f_1 , f_2 , f_2^c , f_3 , f_4 , f_5 , and f_8 —with various permutations of the external legs as arguments. Actually, for f_8 , the authors of [122] considered only the sum of particular solutions to the cut equations: $f_8^{\text{even}} := f_8^+ + f_8^-$, where the superscript indicates the sign of the square root in the solution to the final quadratic cut-equation; for us, both f_8^{even} and $f_8^{\text{odd}} := f_8^+ - f_8^-$ are required. The set of kinematic factors appearing are not all functionally independent; they satisfy the relations also classified in [122].

4.3.1 Integration, Infrared Structure, and Regularization

The particular basis described in ref. [119] has several features that make it promising for loop integration and for exposing critical information about IR-structure of amplitudes. In particular, it is empirically true that prescriptive integrands are often maximally-transcendental and *pure* [41, 42] and thus satisfy canonical, nilpotent differential equations [43, 44, 123]. This should make them comparatively easy to integrate—for example, according to the methods outlined in [43, 124–126]; but perhaps also more directly as illustrated in [127–129].

Another aspect of the basis which may prove valuable is that it was fully divided into infrared-finite and divergent subspaces. This was achieved by choosing as many contours $\{\Omega_J\}$ as possible in the diagonalization (1) to encompass regions responsible for infrared divergences. Moreover, the coefficients of each IR-divergent integral are *manifestly* given by lower-loop expressions; thus, the universal behavior of divergences should be manifested, making it easier to cancel them prior to loop integration. Ideally, we are optimistic that the ratio of different helicity amplitudes could be rendered *locally finite* in the sense of [40] in this basis, but we must leave such questions to future work

(see e.g. [130, 131])

In particular, the MHV amplitude involves 17 and 21 integrands (seed terms for leg-permutation sums) which are manifestly infrared-finite and divergent, respectively; the NMHV amplitude involves 36 finite integrands and 44 divergent integrands.

One final comment is in order regarding regularization. Because the basis of integrands in ref. [119] was defined in strictly four spacetime dimensions and the coefficients \mathbf{a}_J were computed using four-dimensional contours, our integrands are not ensured to give the correct *regulated* expressions if integrated using dimensional regularization: $\mathcal{O}(\epsilon)$ corrections to coefficients can lead to finite corrections to divergent integrals. Nevertheless, we strongly suspect that all regulator dependence will cancel for any finite observable.

Although dimensional regularization is unquestionably the most familiar and most widely used regulator, it is important to note that infrared divergences can be regulated faithfully using massive propagators—by going to the Higgs branch of the theory as in [132, 133]. Importantly, $\mathcal{O}(m^2)$ corrections to integrand coefficients always lead to $\mathcal{O}(m^2)$ contributions to regulated expressions (never canceling a divergence as in ϵ/ϵ in dimensional regularization); as such, our unregulated expressions will yield the correct, regulated results on the Higgs branch.

4.3.2 Consistency Checks

For both the MHV and NMHV amplitudes, the planar parts—the leading (in $1/N_c$) coefficient of $\text{tr}(123456)$ in the expansion of the color-factors—were compared directly against the known results [34, 41]. As these formulae are novel (and non-manifestly dual-conformal) representations of these amplitudes, this is a highly non-trivial check on the correctness of our result.

Beyond the planar limit, it is worth noting that relatively few leading-singularities appear among the contours chosen for the basis. All *other* leading singularities of the amplitude must get matched indirectly in the basis via global residue theorems. Such identities were used to fix all relative signs of terms appearing in these expressions. We have checked that all such residue theorems for both the MHV and NMHV amplitudes are satisfied by our expressions—ensuring that *all* leading singularities of each amplitude are matched.

Chapter 5 | Gauge-Invariant Double-Copies via Recursion

5.1 Tree-Level, On-Shell Recursion for YM and GR

The starting point for on-shell (‘BCFW’) recursion [84] is to consider an amplitude as meromorphic function of external momenta and deform the momenta of any two particles labelled $\{\alpha, \beta\}$ according to

$$p_\alpha \mapsto \hat{p}_\alpha(z) := p_\alpha + z \lambda_\alpha \tilde{\lambda}_\beta, \quad p_\beta \mapsto \hat{p}_\beta(z) := p_\beta - z \lambda_\alpha \tilde{\lambda}_\beta, \quad (5.1)$$

where $p_a =: \lambda_a \tilde{\lambda}_a$ are spinor-helicity variables [134]; this deformation preserves momentum conservation and keeps each particle on-shell. Note that the choice $\{\alpha, \beta\}$ is distinct from the choice $\{\beta, \alpha\}$: they differ by parity. At tree-level, amplitudes have poles at finite z corresponding to factorization channels—the residues of which we may represent diagrammatically as

$$\mathcal{A}_L(\hat{\alpha}^*, \dots, I) \frac{1}{p_L^2} \mathcal{A}_R(I, \dots, \hat{\beta}^*) = \frac{1}{p_L^2} \begin{array}{c} \text{---} \cdots \text{---} \\ | \\ \text{---} \text{---} \text{---} \\ | \\ \hat{\alpha}^* \end{array} \text{---} I \text{---} \begin{array}{c} \text{---} \cdots \text{---} \\ | \\ \text{---} \text{---} \text{---} \\ | \\ \hat{\beta}^* \end{array}, \quad (5.2)$$

where $1/p_L^2$ is the off-shell propagator being cut, with the left/right amplitudes evaluated with $p_{\alpha^*, \beta^*} := p_{\alpha, \beta}(z^*)$ on the location of the pole $z^* = p_L^2 / \langle \alpha | (p_L) | \beta \rangle$ and summed over the states I that can be exchanged. Importantly, the deformed legs must necessarily be on opposite sides of the factorization channel for the simple reason that $\hat{p}_\alpha + \hat{p}_\beta = p_\alpha + p_\beta$ is z -independent.

Provided there are no poles at infinity, Cauchy’s theorem allows us to write an amplitude as a sum over all residues of the form (5.2) [135]. For YM or GR, this will be the case provided the deformed momenta are chosen judiciously according to their helicity

(see e.g. [136]), while amplitudes in maximally supersymmetric ($\mathcal{N}=4$) YM (‘sYM’) or ($\mathcal{N}=8$) GR (‘sGR’) will be free of poles at infinity regardless of which legs are chosen. Because tree-level amplitudes in pure (or any degree of less supersymmetric) YM/GR are identical to those of sYM/sGR for appropriately restricted sets of external states, we may therefore consider the case of maximally supersymmetric YM/GR without loss of generality [137], ensuring that amplitudes are free of poles at infinity for any choice of legs $\{\alpha, \beta\}$.

Notice that the channels (5.2) allow for arbitrary distributions of the other $(n-2)$ legs $A := [n] \setminus \{\alpha, \beta\}$. Thus, on-shell recursion results in a sum of terms of the form

$$\mathcal{A} = \sum_{\substack{\vec{a} \in \mathfrak{S}(A) \\ (\vec{a}_L, \vec{a}_R) = \vec{a}}} \mathcal{A}_L(\widehat{\alpha}^*, \vec{a}_L, I) \frac{1}{p_{\alpha a_L}^2} \mathcal{A}_R(I, \vec{a}_R, \widehat{\beta}^*) =: \sum_{\vec{a} \in \mathfrak{S}(A)} \mathcal{A}(\alpha, \vec{a}, \beta), \quad (5.3)$$

where $\mathcal{A}(\alpha, \vec{a}, \beta) := \mathcal{A}(\alpha, a_1, \dots, a_{-1}, \beta)$ are *partial amplitudes* involving external momenta with *specific ordering*.

As amplitudes in color-dressed YM and gravity are fully permutation-invariant (due to Bose symmetry), any choice of legs $\{\alpha, \beta\}$ may be taken; and any particular ordering of the other legs $\vec{a} \in \mathfrak{S}(A)$ will suffice to generate the full amplitude upon summation over permutations of the labels \vec{a} . Thus we may without loss of generality focus our attention on the determination of the partial amplitude $\mathcal{A}(1, 2, \dots, n-1, n)$.

It is important to note that in *neither theory* is the partial amplitude unique: not only does it depend on the legs chosen, but also the specific sequence of choices made for iterated recursion. (This may seem surprising for YM, as it is common to consider ‘color-stripped’ partial-amplitudes (‘primitives’), which do enjoy many scheme-independent properties.)

One particularly convenient recursion scheme would be to always choose the first and last leg of every iteratively recursed amplitude, and use the same parity of bridge at each stage of recursion. In the case of Yang-Mills, this results in partial amplitudes dressed by the color-factors appearing in the familiar ‘DDM’ representation [120]. Letting $\mathcal{A}^{\text{YM}}(\alpha, \vec{a}, \beta) =: c_{\alpha\beta}^{\vec{a}} A^{\text{YM}}(\alpha, \vec{a}, \beta)$, it is easy to see that the recursion (5.3) separates color and kinematics cleanly so that—upon recursing iteratively down to factorizations involving only three-point amplitudes—we find

$$c_{\alpha\beta}^{\vec{a}} := \sum_{e_i} c^{\alpha, a_1, e_1} c^{e_1, a_2, e_2} \dots c^{e_{-1}, a_{-1}, \beta} \quad (5.4)$$

where c_{ab}^c are the structure constants of some Lie algebra (into which we may freely absorb

Table 5.1: On-shell, gauge-invariant contributions to the 6-point NMHV partial amplitudes of Yang-Mills and gravity. The Grassmann $\delta^{3 \times 4}(C_i \cdot \tilde{\eta})$ appearing in these numerators are defined in (5.17).

Γ_i			
$J(\Gamma_i)$	$s_{61} s_{234} s_{34} D(\Gamma_1)$	$s_{61} s_{23} s_{45} D(\Gamma_2)$	$s_{61} s_{345} s_{34} D(\Gamma_3)$
$D(\Gamma_i)$	$s_{56} \frac{\langle 1 (2) (34) 5 \rangle \langle 1 (23) (4) (3) 2 \rangle}{\langle 15 \rangle \langle 1 (43) 2 \rangle}$	$s_{123} \frac{\langle 1 (2) (3) (45) 6 \rangle \langle 1 (23) (4) (5) 6 \rangle}{\langle 1 (23) 6 \rangle \langle 1 (45) 6 \rangle}$	$s_{12} \frac{[2 (34) (5) 6] \langle 5 (4) (3) (45) 6 \rangle}{[26] \langle 5 (34) 6 \rangle}$
$n(\Gamma_i)$	$\frac{\langle 12 \rangle [34] [56] \delta^{3 \times 4}(C_3 \cdot \tilde{\eta})}{s_{234} \langle 1 (56) 2 \rangle [34] \langle 51 \rangle \langle 61 \rangle}$	$\frac{[23] \langle 45 \rangle \delta^{3 \times 4}(C_5 \cdot \tilde{\eta})}{\langle 1 (23) 6 \rangle^2 [45] \langle 23 \rangle}$	$\frac{\langle 12 \rangle [34] [56] \delta^{3 \times 4}(C_1 \cdot \tilde{\eta})}{s_{345} \langle 5 (34) 6 \rangle [34] [26] [61]}$

any coupling constant), and $\{a, b, c\}$ are (adjoint) color-labels for the gluons. These color tensors are all independent under Jacobi-relations, and the so-called ‘primitive’ ordered amplitudes of YM turn out to be gauge-invariant, local, dihedrally symmetric, and to enjoy KK relations. (All of these properties can be deduced from the Jacobi identity and Bose symmetry of color-dressed amplitudes alone.) Besides gauge-invariance, none of these properties will be enjoyed by the partial amplitudes of gravity—the meaning of which will depend strongly on how recursion is implemented (analogously to color tensors for YM).

Because this recursion scheme results in the same color-factor $c_{\alpha\beta}^{\vec{a}}$ coefficient for every term, it is common to factor it out entirely and focus on the *color-stripped* partial amplitude primitive $A^{\text{YM}}(1, 2, \dots, n-1, n)$.

5.2 On-Shell Diagrammatics of YM and GR

For color-stripped partial amplitudes in YM, there exists a powerful diagrammatic manifestation of recursion relations following from the simple fact that

$$\frac{1}{p_{12\dots j}^2} \text{YM} \text{---} \text{YM} = \text{YM} \quad (5.5)$$

Here, we have introduced ‘flat’ vertices to denote *ordered* partial amplitude primitives. The right hand side represents an *on-shell function* of YM: the product of (color-stripped) amplitudes at the vertices, summing over all the on-shell, internal states that can be exchanged between them. These functions are extremely well understood: they are

classified combinatorially, and all their functional relations can be understood to arise homologically from an auxiliary Grassmannian ‘positive’ geometry (see e.g. [16, 98]).

Applying recursion successively results in a representation of color-stripped YM partial amplitudes as sums over on-shell functions encoded by *specific* on-shell diagrams $\{\Gamma\}$

$$A^{\text{YM}}(1, 2, \dots, n-1, n) = \sum_{\Gamma} \mathfrak{f}_{\Gamma}^{\text{YM}} =: \sum_{\Gamma} \widehat{\mathfrak{f}}_{\Gamma}^{\text{YM}} \delta^{2 \times 2}(\lambda \cdot \widetilde{\lambda}) \quad (5.6)$$

where the sum is over on-shell diagrams $\{\Gamma\}$ of the form (5.5) involving *exclusively* three-point vertices. The N^k MHV-degree of an amplitude is encoded by the graph according to $k=2n_B+n_W-n_I-2$, where $n_B(n_W)$ denotes the number of blue(white) vertices and n_I the number of internal lines. Even for MHV amplitudes, there are vastly more on-shell *diagrams* than on-shell functions—as diagrams related by mergers and square moves leave on-shell functions unchanged *in YM* [98]. On-shell diagrams in gravity enjoy only the square move as an (un-modified) equivalence relation [99].

5.3 Color-Kinematic *Denominators* for Gravity

For amplitudes in GR, there is no simple analogue of (5.5) (see e.g. [99, 100]); but, supposing that there is some diagrammatic representation for partial amplitudes in GR in terms of on-shell diagrams of YM, we may recursively conclude that

$$\begin{aligned} \frac{1}{p_L^2} \left(\text{Diagram}_{\text{GR}}^L \text{---} \text{Diagram}_{\text{GR}}^R \right) &= p_L^2 J(\Gamma_L) J(\Gamma_R) \left(\frac{1}{p_L^2} \left(\text{Diagram}_{\text{YM}}^L \text{---} \text{Diagram}_{\text{YM}}^R \right) \right)^2 \\ &=: D(\Gamma) (\widehat{\mathfrak{f}}_{\Gamma}^{\text{YM}})^2 \delta^{2 \times 2}(\lambda \cdot \widetilde{\lambda}). \end{aligned} \quad (5.7)$$

The fact that BCFW recursion for GR can be expressed in the form (5.7) is reasonably well known [99–103]. The precise form of $D(\Gamma)$ depends both on the graph Γ and the recursion scheme followed. If we always choose the first and last labels for subsequent recursion, so that every diagram appearing is of the form $\Gamma_{\alpha\beta}^{\vec{a}} = \Gamma_L[\widehat{\alpha}^*, \vec{a}_L, I] \otimes \Gamma_R[I, \vec{a}_R, \widehat{\beta}^*]$, then $D(\Gamma)$ will be

$$D\left(\Gamma_{\alpha\beta}^{\vec{a}}\right) = p_{\alpha a_L}^2 D\left(\Gamma_{\widehat{\alpha}^* I}^{\vec{a}_L}\right) D\left(\Gamma_{I \widehat{\beta}^*}^{\vec{a}_R}\right). \quad (5.8)$$

We call these factors color-kinematic *denominators* because if we let $n(\Gamma) := D(\Gamma) \widehat{\mathfrak{f}}_{\Gamma}^{\text{YM}}$ then individual terms appearing in the recursion of an amplitude in YM take the form

$$\frac{c_{\alpha\beta}^{\vec{a}} n\left(\Gamma_{\alpha\beta}^{\vec{a}}\right)}{D\left(\Gamma_{\alpha\beta}^{\vec{a}}\right)} = c_{\alpha\beta}^{\vec{a}} \widehat{\mathfrak{f}}_{\Gamma_{\alpha\beta}^{\vec{a}}}^{\text{YM}} \quad (5.9)$$

while terms in gravity are given by the *double-copy*

$$\frac{n(\Gamma_{\alpha\beta}^{\vec{a}}) n(\Gamma_{\alpha\beta}^{\vec{a}})}{D(\Gamma_{\alpha\beta}^{\vec{a}})} = D(\Gamma_{\alpha\beta}^{\vec{a}}) (\hat{f}_{\Gamma_{\alpha\beta}^{\vec{a}}}^{\text{YM}})^2. \quad (5.10)$$

5.4 Illustrations of On-Shell Double-Copies

Arguably the simplest amplitudes in either theory are the so-called ($N^{k=0}$)MHV amplitudes [93, 97, 138]. On-shell recursion results in a single term for ordered partial amplitudes in either theory:

$$\begin{aligned} \mathcal{A}_{\text{MHV}}^{\text{YM}}(1, \dots, n) &= c_{1n}^{\vec{a}} \frac{\delta^{2 \times 4}(\lambda \cdot \tilde{\eta}) \delta^{2 \times 2}(\lambda \cdot \tilde{\lambda})}{\langle 12 \rangle \langle 23 \rangle \dots \langle n-1 n \rangle \langle n1 \rangle} \\ &=: c_{1n}^{\vec{a}} \frac{n(\Gamma_{1n}^{\text{MHV}})}{D(\Gamma_{1n}^{\text{MHV}})} \delta^{2 \times 2}(\lambda \cdot \tilde{\lambda}) =: c_{1n}^{\vec{a}} \text{PT}(1 \dots n) \delta^{2 \times 2}(\lambda \cdot \tilde{\lambda}), \end{aligned} \quad (5.11)$$

where the denominators are determined recursively. In the default recursion scheme (5.8), we find

$$\begin{aligned} D(\Gamma_{1n}^{\text{MHV}}) &:= p_{n-1n}^2 \prod_{j=4}^{n-1} \frac{\langle 1|(2 \dots j-2)|(j-1)|j \rangle}{\langle 1j \rangle}, \\ n(\Gamma_{1n}^{\text{MHV}}) &:= D(\Gamma_{1n}^{\text{MHV}}) \frac{\delta^{2 \times 4}(\lambda \cdot \tilde{\eta})}{\langle 12 \rangle \langle 23 \rangle \dots \langle n-1 n \rangle \langle n1 \rangle} \\ &= \frac{[32]}{\langle 23 \rangle \langle n1 \rangle^2} \prod_{j=4}^{n-1} \frac{\langle 1|(2 \dots j-1)|j \rangle}{\langle 1j \rangle} \delta^{2 \times 4}(\lambda \cdot \tilde{\eta}); \end{aligned} \quad (5.12)$$

this representation immediately allows us to write the corresponding expressions for GR as a double-copy:

$$\begin{aligned} \mathcal{A}_{\text{MHV}}^{\text{GR}}(1, \dots, n) &= \frac{n(\Gamma_{1n}^{\text{MHV}}) n(\Gamma_{1n}^{\text{MHV}})}{D(\Gamma_{1n}^{\text{MHV}})} \delta^{2 \times 2}(\lambda \cdot \tilde{\lambda}) \\ &= D(\Gamma_{1n}^{\text{MHV}}) (\text{PT}(1 \dots n))^2 \delta^{2 \times 2}(\lambda \cdot \tilde{\lambda}). \end{aligned} \quad (5.13)$$

Unlike the case of YM, these partial amplitudes in GR are non-cyclic and involve non-local poles. Only upon summing over all $(n-2)!$ orderings of $\{2, \dots, n-1\}$ do we recover a local, permutation-invariant amplitude. We have checked that this formula agrees with the closed-form expression of Hodges [139] through $n=12$ particles.

It is worth noting that this representation of MHV amplitudes in gravity (5.13) is *identical* (upon a rotation of labels) to that found in [90]. And as with [90], the use of the ‘bonus relations’ stemming from the good large- z behavior of amplitudes in GR [137] allows us to re-write (5.13) as a sum over $(n-3)!$ terms [89]:

Table 5.3: Alternative recursion schemata resulting in distinct ordered, partial amplitudes $\mathcal{A}^{\text{GR}}(1, 2, 3, 4, 5, 6)$.

Γ_i				
$J(\Gamma_i)$	$s_{61} s_{23} s_{234} D(\Gamma_a)$	$s_{61} s_{34} s_{234} D(\Gamma_b)$	$s_{61} s_{34} s_{345} D(\Gamma_c)$	$s_{61} s_{23} s_{345} D(\Gamma_d)$
$D(\Gamma_i)$	$s_{56} \frac{\langle 1(2)(3)4 \rangle \langle 1(23)(4)5 \rangle}{\langle 14 \rangle \langle 15 \rangle}$	$s_{56} \frac{\langle 2(3)(4)5 \rangle \langle 1(2)(34)5 \rangle}{\langle 25 \rangle \langle 15 \rangle}$	$s_{12} \frac{\langle 2(3)(4)5 \rangle \langle 2(34)(5)6 \rangle}{\langle 25 \rangle \langle 26 \rangle}$	$s_{12} \frac{\langle 2(3)(45)6 \rangle \langle 3(4)(5)6 \rangle}{\langle 26 \rangle \langle 36 \rangle}$
$n(\Gamma_i)$	$\frac{\langle 1(23)4 \rangle \langle 23 \rangle \langle 56 \rangle}{\langle 14 \rangle \langle 15 \rangle \langle 23 \rangle \langle 61 \rangle} \delta^{2 \times 4}(\lambda, \tilde{\eta})$	$\frac{\langle 5(34)2 \rangle \langle 34 \rangle \langle 56 \rangle}{\langle 15 \rangle \langle 25 \rangle \langle 34 \rangle \langle 61 \rangle} \delta^{2 \times 4}(\lambda, \tilde{\eta})$	$\frac{\langle 2(34)5 \rangle \langle 12 \rangle \langle 34 \rangle}{\langle 25 \rangle \langle 26 \rangle \langle 34 \rangle \langle 61 \rangle} \delta^{2 \times 4}(\lambda, \tilde{\eta})$	$\frac{\langle 6(45)3 \rangle \langle 12 \rangle \langle 45 \rangle}{\langle 26 \rangle \langle 36 \rangle \langle 45 \rangle \langle 61 \rangle} \delta^{2 \times 4}(\lambda, \tilde{\eta})$

$$\hat{\mathcal{A}}_{\text{MHV}}^{\text{GR}} = \sum_{\vec{a} \in \mathfrak{S}(3, \dots, n-1)} \frac{\langle n1 \rangle \langle 23 \rangle}{\langle n2 \rangle \langle 13 \rangle} D(\Gamma_{1\vec{a}}) (\text{PT}(12\vec{a}n))^2. \quad (5.14)$$

For higher $N^{k>0}$ MHV-degrees, on-shell recursion typically involves a sum over terms, each represented in YM by a particular, primitive on-shell diagram. The simplest non-trivial example is the 6-particle NMHV amplitude, which involves 3 terms to represent the ordered amplitude. Following the recursion scheme described above, the three on-shell diagrams $\{\Gamma_1, \Gamma_2, \Gamma_3\}$ that result are given in Table 5.1, where we have also indicated the numerators $n(\Gamma_i)$ and denominators $D(\Gamma_i)$ of each. Thus, we may write the ordered, partial NMHV amplitude primitive in YM as

$$\mathcal{A}_{6,1}^{\text{YM}}(1, \dots, n) = c_{16}^{\vec{a}} \left(\frac{n(\Gamma_1)}{D(\Gamma_1)} + \frac{n(\Gamma_2)}{D(\Gamma_2)} + \frac{n(\Gamma_3)}{D(\Gamma_3)} \right) \delta^{2 \times 2}(\lambda, \tilde{\lambda}) \quad (5.15)$$

and the corresponding partial amplitude in GR as the double-copy

$$\mathcal{A}_{6,1}^{\text{GR}}(1, \dots, n) = \left(\frac{n(\Gamma_1)^2}{D(\Gamma_1)} + \frac{n(\Gamma_2)^2}{D(\Gamma_2)} + \frac{n(\Gamma_3)^2}{D(\Gamma_3)} \right) \delta^{2 \times 2}(\lambda, \tilde{\lambda}). \quad (5.16)$$

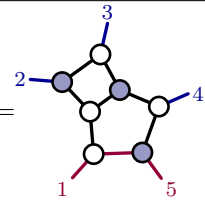
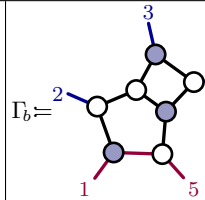
In both cases, these partial amplitudes must be summed over the $(n-2)!$ orderings of the legs $\{2, \dots, 5\}$. We have checked this expression against KLT [140].

The numerators listed in Table 5.1 involve Grassmann δ -functions involving the $\tilde{\eta}$'s which label the external states of each supermultiplet [137]; they are defined by

$$\begin{aligned} \delta^{3 \times 4}(C_a \cdot \tilde{\eta}) &:= \\ \delta^{2 \times 4}(\lambda \cdot \tilde{\eta}) \delta^{1 \times 4}([a+1] \tilde{\eta}_{a-1} + [a+1 \ a-1] \tilde{\eta}_a + [a-1 \ a] \tilde{\eta}_{a+1}). \end{aligned} \quad (5.17)$$

Notice that $\delta^{3 \times 4}(C_a \cdot \tilde{\eta})$ is invariant under permutations of both the set $\{a-1, a, a+1\}$ and its complement. This will turn out to have important consequences as we discuss in the

Table 5.2: Alternative recursion schemata resulting in distinct ordered, partial amplitudes ‘ $\mathcal{A}^{\text{GR}}(1, 2, 3, 4, 5)$ ’.

Γ_i	$\Gamma_a \equiv$ 	$\Gamma_b \equiv$ 
$J(\Gamma_i)$	$s_{51} s_{23} D(\Gamma_a)$	$s_{51} s_{34} D(\Gamma_b)$
$D(\Gamma_i)$	$s_{45} \frac{\langle 1 2\rangle\langle 3 4\rangle}{\langle 14\rangle}$	$s_{12} \frac{\langle 2 3\rangle\langle 4 5\rangle}{\langle 25\rangle}$
$n(\Gamma_i)$	$\frac{[23][45]}{\langle 14\rangle\langle 23\rangle\langle 51\rangle} \delta^{2 \times 4}(\lambda \cdot \tilde{\eta})$	$\frac{[12][34]}{\langle 34\rangle\langle 25\rangle\langle 51\rangle} \delta^{2 \times 4}(\lambda \cdot \tilde{\eta})$

forthcoming work [141].

Although the expression (5.15) may seem unusual, it is worth observing that, for example,

$$\frac{n(\Gamma_2)}{D(\Gamma_2)} = \frac{\delta^{2 \times 4}(\lambda \cdot \tilde{\eta}) \delta^{1 \times 4}([56]\tilde{\eta}_4 + [64]\tilde{\eta}_5 + [45]\tilde{\eta}_6)}{[56]\langle 12\rangle\langle 3|(45)|6\rangle s_{123} [4|(56)1]\langle 23\rangle[45]}, \quad (5.18)$$

is simply the (momentum-space version of the) familiar R -invariant $\mathcal{R}[1, 3, 4, 5, 6]$ (see e.g. [9]).

Up to minor conventional differences, the recursion scheme used to construct denominators (5.8) generally reproduces the form of amplitudes in GR as they were derived in [91]. We have implemented in this in MATHEMATICA and have verified agreement against KLT [140] through the 10-particle $N^3\text{MHV}$ amplitude. These tools will be made available in a forthcoming, public package for tree amplitudes more generally [142] (see also [143]).

5.5 Non-Uniqueness of Dual Denominators

As emphasized above, even restricting ourselves to successively choosing the first last legs for all iterated recursions, variability emerges from the chiral asymmetry of the BCFW deformation (5.1). Even for 5 particles, choosing $\{\alpha, \beta\}$ to be $\{1, 5\}$ versus $\{5, 1\}$ (conjugating the shifting rule) results in two distinct diagrams Γ_a and Γ_b and correspondingly *distinct* primitives $n(\Gamma_i)^2/D(\Gamma_i)$

$$\mathcal{A}_a^{\text{GR}}(1, \dots, 5) := \frac{\langle 1|(2)|(3)|4\rangle[45] \delta^{2 \times 8}(\lambda \cdot \tilde{\eta})}{\langle 14\rangle\langle 45\rangle(\langle 12\rangle\langle 23\rangle\langle 34\rangle\langle 51\rangle)^2} \delta^{2 \times 2}(\lambda \cdot \tilde{\lambda});$$

$$\mathcal{A}_b^{\text{GR}}(1, \dots, 5) := \frac{\langle 2|(3)|(4)|5\rangle[12] \delta^{2 \times 8}(\lambda \cdot \tilde{\eta})}{\langle 12\rangle\langle 25\rangle(\langle 23\rangle\langle 34\rangle\langle 45\rangle\langle 51\rangle)^2} \delta^{2 \times 2}(\lambda \cdot \tilde{\lambda}).$$

Nevertheless, it is easy to verify that the sum over their permuted images agree:

$$\mathcal{A}^{\text{GR}} = \sum_{\vec{a} \in \mathfrak{S}([2, \dots, 4])} \mathcal{A}_a^{\text{GR}}(\mathbf{1}, a_1, \dots, a_{-1}, 5) = \sum_{\vec{a} \in \mathfrak{S}([2, \dots, 4])} \mathcal{A}_b^{\text{GR}}(\mathbf{1}, a_1, \dots, a_{-1}, 5).$$

This variability only proliferates for higher multiplicity, as evidenced by the four examples for 6-point MHV given in Table 5.3. More generally, the equivalence of expressions upon distinct variations gives powerful identities among not merely the partial amplitudes in YM, but even among individual on-shell functions appearing in $N^{k>0}$ MHV amplitudes. We will explore the scope of these possibilities and their consequences in a forthcoming work [141].

Chapter 6 |

Conclusions and Future Directions

In this work, we have constructed a diagonal basis of four-dimensional local loop integrands with triangle power-counting at two loops and six particles. As we have emphasized, the properties of this basis are entirely dependent on the choice of eight-dimensional compact contours on which the integrands are normalized to be unit. The specific choices in this paper amount to making infrared structure, polylogarithmicity, and purity as manifest as possible; this is important for practical applications including carrying out the loop integrals, since uniformly transcendental integrals obey particularly simple differential equations [43, 124–126], among other nice properties [41]. Of course, integrating the basis of this paper in dimensional regularization requires (at least for those elements with infrared divergences) the addition of the extra-dimensional terms relevant for $d=4-2\epsilon$ dimensions. In addition to this, we expect the finite part of our basis to be an ideal testing ground for testing the methods of direct integration [128, 129] in the non-planar sector.

This basis is sufficient to express the six-particle MHV and NMHV amplitudes in both sYM and SUGRA, and doing so requires only the computation of the physical leading singularities which are among the spanning set chosen in this work. It should be relatively straightforward to compute the relevant fully color-dressed leading singularities in sYM.

Because the basis of integrands is identical for both MHV and NMHV helicity configurations, having representations of both amplitude integrands in hand immediately suggests an obvious application: namely, the study of non-planar versions of the two-loop ratio function. The universal nature of the infrared divergence of non-planar amplitudes strongly suggests that the ratio of the NMHV and MHV amplitudes should define a *locally-finite* quantity according to the definition of [40], but due to the presence of color factors, the details of how this works remain unclear.

Another natural extension of this work would be to consider bubble or worse degrees of power-counting. Although this introduces new degrees of freedom and higher poles at infinity, because $\mathfrak{B}_p \subset \mathfrak{B}_q$ for any $p > q$, *every* contour used in the basis constructed in this work can be recycled and used to fill out a large subset of the spanning set of contours for bubble power-counting (and beyond). Note that while the integrands will be modified by both additional top-level and contact term numerators, the contours themselves require no modification whatsoever.

Instead of boosting the power-counting, implementing the diagonalization procedure of this work at higher multiplicities and higher loops offers an additional direction for future investigations. Generating diagonal bases beyond this work will inevitably require non-polylogarithmic contours and integrands [53, 54]; here, we expect the extension of prescriptive unitarity to elliptic (and beyond) leading singularities outlined in [39] to prove quite useful.

The integration of non-planar Feynman integrands involving six particles is at or arguably just beyond our present state of the art. Indeed, it was only recently that the first non-planar amplitudes (in maximally supersymmetric theories) were computed for five-particles [144–147]. In this work we have provided explicit representations of both the NMHV and MHV six particle amplitude in precisely the same prescriptive basis of integrands—engineered to simplify the work of loop integration and to maximally expose the infrared structure of each amplitude. We suspect that there exists some non-planar analogue of the IR-finite ratio function of planar theories, and the first non-trivial instance of such should appear for six particles. Once the integrated expressions are found for these integrands, we anticipate the discovery of simplifications as dramatic as for in the case of planar amplitudes (see e.g. [48, 49])—and we hope that these will lead to similarly powerful new insights for amplitudes beyond the planar limit.

The number of terms generated by BCFW to represent the n -particle N^k MHV amplitude for a specific ordering is given by a Narayana number $\frac{1}{n-3} \binom{n-3}{k+1} \binom{n-3}{k}$. It is natural to suppose that including a sum over $(n-2)!$ permutations of leg labels would result in as many more terms in the expression for gravity. This turns out to not be the case—as evidenced, for example, by the more compact expression for MHV amplitudes (5.14).

Interestingly, for higher multiplicity and N^k MHV-degree, considerations of Grassmannian geometry of the $\tilde{\eta}$ -coefficients expose *even more* symmetry than would result from mere permutation-invariance of amplitudes in GR [141]. For the 10-particle N^3 MHV amplitude, for example, we require only 343,252 distinct superfunctions—about 20 times

fewer than the naïve estimate of $(175 \times 8!)$. Moreover, the contributions that appear are found to satisfy a number of novel functional relations—some of which can be demonstrated using bonus relations or by equating formulae resulting from different recursion schemata, but we have also stumbled into yet further relations that remain to be understood. We explore some of these aspects of gravitational amplitudes in [141]. This additional, geometric structure hints at the possibility of a broader geometric story, perhaps analogous to the ‘gravituhedron’ described in [102].

While the existence of color-kinematic dual numerators remains conjectural beyond tree-level, there is a great deal of evidence from specific examples that the double-copy should generalize to loop-integrands (in some form or other) [30, 66–68, 148–150]. In ref. [99], Heslop and Lipstein gave evidence at one loop that the obvious extension of on-shell recursion for loop-integrands for sYM [6] works also for sGR. It is natural to wonder if this works more generally, and if loop amplitude integrands for sGR continue to be generated as a double-copy of those for color-dressed sYM.

Bibliography

- [1] Z. Bern, L. J. Dixon, D. C. Dunbar and D. A. Kosower, *One-Loop n -Point Gauge Theory Amplitudes, Unitarity and Collinear Limits*, *Nucl. Phys.* **B425** (1994) 217–260, [[hep-ph/9403226](#)].
- [2] Z. Bern, L. J. Dixon, D. C. Dunbar and D. A. Kosower, *Fusing Gauge Theory Tree Amplitudes into Loop Amplitudes*, *Nucl. Phys.* **B435** (1995) 59–101, [[hep-ph/9409265](#)].
- [3] R. Britto, F. Cachazo and B. Feng, *Generalized Unitarity and One-Loop Amplitudes in $\mathcal{N}=4$ Super-Yang-Mills*, *Nucl. Phys.* **B725** (2005) 275–305, [[hep-th/0412103](#)].
- [4] R. Britto, F. Cachazo and B. Feng, *New Recursion Relations for Tree Amplitudes of Gluons*, *Nucl. Phys.* **B715** (2005) 499–522, [[hep-th/0412308](#)].
- [5] R. Britto, F. Cachazo, B. Feng and E. Witten, *Direct Proof of Tree-Level Recursion Relation in Yang-Mills Theory*, *Phys. Rev. Lett.* **94** (2005) 181602, [[hep-th/0501052](#)].
- [6] N. Arkani-Hamed, J. L. Bourjaily, F. Cachazo, S. Caron-Huot and J. Trnka, *The All-Loop Integrand For Scattering Amplitudes in Planar $\mathcal{N}=4$ SYM*, *JHEP* **1101** (2011) 041, [[1008.2958](#)].
- [7] J. Drummond, J. Henn, V. Smirnov and E. Sokatchev, *Magic Identities for Conformal Four-Point Integrals*, *JHEP* **0701** (2007) 064, [[hep-th/0607160](#)].
- [8] L. F. Alday and J. M. Maldacena, *Gluon Scattering Amplitudes at Strong Coupling*, *JHEP* **06** (2007) 064, [[0705.0303](#)].
- [9] J. Drummond, J. Henn, G. Korchemsky and E. Sokatchev, *Dual Superconformal Symmetry of Scattering Amplitudes in $\mathcal{N}=4$ super Yang-Mills Theory*, *Nucl. Phys.* **B828** (2010) 317–374, [[0807.1095](#)].
- [10] J. M. Drummond, J. M. Henn and J. Plefka, *Yangian Symmetry of Scattering Amplitudes in $\mathcal{N}=4$ Super Yang-Mills Theory*, *JHEP* **05** (2009) 046, [[0902.2987](#)].
- [11] N. Arkani-Hamed, J. Bourjaily, F. Cachazo and J. Trnka, *Local Spacetime Physics from the Grassmannian*, *JHEP* **1101** (2011) 108, [[0912.3249](#)].

- [12] N. Arkani-Hamed, J. Bourjaily, F. Cachazo and J. Trnka, *Unification of Residues and Grassmannian Dualities*, *JHEP* **1101** (2011) 049, [[0912.4912](#)].
- [13] J. Kaplan, *Unraveling $\mathcal{L}_{n,k}$: Grassmannian Kinematics*, *JHEP* **1003** (2010) 025, [[0912.0957](#)].
- [14] J. L. Bourjaily, J. Trnka, A. Volovich and C. Wen, *The Grassmannian and the Twistor String: Connecting All Trees in $\mathcal{N}=4$ SYM*, *JHEP* **1101** (2011) 038, [[1006.1899](#)].
- [15] N. Arkani-Hamed, J. L. Bourjaily, F. Cachazo, A. B. Goncharov, A. Postnikov and J. Trnka, *Scattering Amplitudes and the Positive Grassmannian*, [1212.5605](#).
- [16] J. L. Bourjaily, *Positroids, Plabic Graphs, and Scattering Amplitudes in MATHEMATICA*, [1212.6974](#).
- [17] N. Arkani-Hamed, J. L. Bourjaily, F. Cachazo, A. Postnikov and J. Trnka, *On-Shell Structures of MHV Amplitudes Beyond the Planar Limit*, *JHEP* **06** (2015) 179, [[1412.8475](#)].
- [18] N. Arkani-Hamed, J. L. Bourjaily, F. Cachazo, A. Hodges and J. Trnka, *A Note on Polytopes for Scattering Amplitudes*, *JHEP* **1204** (2012) 081, [[1012.6030](#)].
- [19] N. Arkani-Hamed and J. Trnka, *The Amplituhedron*, *JHEP* **1410** (2014) 30, [[1312.2007](#)].
- [20] N. Arkani-Hamed and J. Trnka, *Into the Amplituhedron*, *JHEP* **1412** (2014) 182, [[1312.7878](#)].
- [21] J. L. Bourjaily, E. Herrmann, C. Langer and J. Trnka, *Building Bases of Loop Integrands*, *JHEP* **11** (2020) 116, [[2007.13905](#)].
- [22] Z. Bern, J. Rozowsky and B. Yan, *Two-Loop Four-Gluon Amplitudes in $\mathcal{N}=4$ SuperYang-Mills*, *Phys. Lett.* **B401** (1997) 273–282, [[hep-ph/9702424](#)].
- [23] N. Arkani-Hamed, J. L. Bourjaily, F. Cachazo and J. Trnka, *Singularity Structure of Maximally Supersymmetric Scattering Amplitudes*, *Phys. Rev. Lett.* **113** (2014) 261603, [[1410.0354](#)].
- [24] Z. Bern, L. J. Dixon and R. Roiban, *Is $\mathcal{N}=8$ Supergravity Ultraviolet Finite?*, *Phys. Lett.* **B644** (2007) 265–271, [[hep-th/0611086](#)].
- [25] Z. Bern, J. Carrasco, L. J. Dixon, H. Johansson, D. Kosower et al., *Three-Loop Superfiniteness of $\mathcal{N}=8$ Supergravity*, *Phys. Rev. Lett.* **98** (2007) 161303, [[hep-th/0702112](#)].
- [26] Z. Bern, J. J. M. Carrasco, L. J. Dixon, H. Johansson and R. Roiban, *Manifest Ultraviolet Behavior for the Three-Loop Four-Point Amplitude of $\mathcal{N}=8$ Supergravity*, *Phys. Rev. D* **78** (2008) 105019, [[0808.4112](#)].

- [27] Z. Bern, J. Carrasco, L. J. Dixon, H. Johansson and R. Roiban, *The Ultraviolet Behavior of $\mathcal{N}=8$ Supergravity at Four Loops*, *Phys. Rev. Lett.* **103** (2009) 081301, [[0905.2326](#)].
- [28] Z. Bern, J. Carrasco, L. J. Dixon, H. Johansson and R. Roiban, *The Complete Four-Loop Four-Point Amplitude in $\mathcal{N}=4$ Super-Yang-Mills Theory*, *Phys. Rev.* **D82** (2010) 125040, [[1008.3327](#)].
- [29] Z. Bern, J. J. M. Carrasco, W.-M. Chen, H. Johansson, R. Roiban and M. Zeng, *The Five-Loop Four-Point Integrand of $\mathcal{N}=8$ Supergravity as a Generalized Double Copy*, *Phys. Rev. D* **96** (2017) 126012, [[1708.06807](#)].
- [30] J. J. M. Carrasco and H. Johansson, *Five-Point Amplitudes in $\mathcal{N}=4$ Super-Yang-Mills Theory and $\mathcal{N}=8$ Supergravity*, *Phys. Rev.* **D85** (2012) 025006, [[1106.4711](#)].
- [31] J. L. Bourjaily, E. Herrmann, C. Langer, A. J. McLeod and J. Trnka, *Prescriptive Unitarity for Non-Planar Six-Particle Amplitudes at Two Loops*, *JHEP* **12** (2019) 073, [[1909.09131](#)].
- [32] J. L. Bourjaily, E. Herrmann, C. Langer, A. J. McLeod and J. Trnka, *All-Multiplicity Nonplanar Amplitude Integrands in Maximally Supersymmetric Yang-Mills Theory at Two Loops*, *Phys. Rev. Lett.* **124** (2020) 111603, [[1911.09106](#)].
- [33] J. L. Bourjaily, S. Caron-Huot and J. Trnka, *Dual-Conformal Regularization of Infrared Loop Divergences and the Chiral Box Expansion*, *JHEP* **1501** (2015) 001, [[1303.4734](#)].
- [34] J. L. Bourjaily and J. Trnka, *Local Integrand Representations of All Two-Loop Amplitudes in Planar SYM*, *JHEP* **08** (2015) 119, [[1505.05886](#)].
- [35] J. L. Bourjaily, E. Herrmann and J. Trnka, *Prescriptive Unitarity*, *JHEP* **06** (2017) 059, [[1704.05460](#)].
- [36] J. L. Bourjaily, A. DiRe, A. Shaikh, M. Spradlin and A. Volovich, *The Soft-Collinear Bootstrap: $\mathcal{N}=4$ Yang-Mills Amplitudes at Six and Seven Loops*, *JHEP* **1203** (2012) 032, [[1112.6432](#)].
- [37] J. L. Bourjaily, P. Heslop and V.-V. Tran, *Perturbation Theory at Eight Loops: Novel Structures and the Breakdown of Manifest Conformality in $\mathcal{N}=4$ Supersymmetric Yang-Mills Theory*, *Phys. Rev. Lett.* **116** (2016) 191602, [[1512.07912](#)].
- [38] J. L. Bourjaily, P. Heslop and V.-V. Tran, *Amplitudes and Correlators to Ten Loops Using Simple, Graphical Bootstraps*, *JHEP* **11** (2016) 125, [[1609.00007](#)].

- [39] J. L. Bourjaily, N. Kalyanapuram, C. Langer and K. Patatoukos, *Prescriptive Unitarity with Elliptic Leading Singularities*, *Phys. Rev. D* **104** (2021) 125009, [[2102.02210](#)].
- [40] J. L. Bourjaily, C. Langer and K. Patatoukos, *Locally-Finite Quantities in sYM*, *JHEP* **04** (2021) 298, [[2102.02821](#)].
- [41] N. Arkani-Hamed, J. L. Bourjaily, F. Cachazo and J. Trnka, *Local Integrals for Planar Scattering Amplitudes*, *JHEP* **1206** (2012) 125, [[1012.6032](#)].
- [42] J. M. Drummond, J. M. Henn and J. Trnka, *New Differential Equations for On-Shell Loop Integrals*, *JHEP* **1104** (2011) 083, [[1010.3679](#)].
- [43] J. M. Henn, *Multiloop Integrals in Dimensional Regularization Made Simple*, *Phys. Rev. Lett.* **110** (2013) 251601, [[1304.1806](#)].
- [44] J. Broedel, C. Duhr, F. Dulat, B. Penante and L. Tancredi, *Elliptic Feynman Integrals and Pure Functions*, *JHEP* **01** (2019) 023, [[1809.10698](#)].
- [45] J. L. Bourjaily, E. Herrmann and J. Trnka, *Amplitudes at Infinity*, *Phys. Rev. D* **99** (2019) 066006, [[1812.11185](#)].
- [46] Z. Bern, L. J. Dixon, D. A. Kosower, R. Roiban, M. Spradlin, C. Vergu and A. Volovich, *The Two-Loop Six-Gluon MHV Amplitude in Maximally Supersymmetric Yang-Mills Theory*, *Phys. Rev. D* **78** (2008) 045007, [[0803.1465](#)].
- [47] D. Kosower, R. Roiban and C. Vergu, *The Six-Point NMHV amplitude in Maximally Supersymmetric Yang-Mills Theory*, *Phys. Rev. D* **83** (2011) 065018, [[1009.1376](#)].
- [48] V. Del Duca, C. Duhr and V. A. Smirnov, *An Analytic Result for the Two-Loop Hexagon Wilson Loop in $N = 4$ SYM*, *JHEP* **03** (2010) 099, [[0911.5332](#)].
- [49] A. B. Goncharov, M. Spradlin, C. Vergu and A. Volovich, *Classical Polylogarithms for Amplitudes and Wilson Loops*, *Phys. Rev. Lett.* **105** (2010) 151605, [[1006.5703](#)].
- [50] J. L. Bourjaily, C. Langer and Y. Zheng, “The Two-Loop, Color-Dressed, Six-Point NMHV Amplitude Integrand.”
- [51] J. L. Bourjaily, A. J. McLeod, M. von Hippel and M. Wilhelm, *A (Bounded) Bestiary of Feynman Integral Calabi-Yau Geometries*, *Phys. Rev. Lett.* **122** (2019) 031601, [[1810.07689](#)].
- [52] J. L. Bourjaily, N. Kalyanapuram, C. Langer, K. Patatoukos and M. Spradlin, *An Elliptic, Yangian-Invariant ‘Leading Singularity’*, *Phys. Rev. Lett.* **126** (2021) 201601, [[2012.14438](#)].

- [53] J. L. Bourjaily, A. J. McLeod, M. Spradlin, M. von Hippel and M. Wilhelm, *Elliptic Double-Box Integrals: Massless Scattering Amplitudes beyond Polylogarithms*, *Phys. Rev. Lett.* **120** (2018) 121603, [[1712.02785](#)].
- [54] J. L. Bourjaily, Y.-H. He, A. J. McLeod, M. von Hippel and M. Wilhelm, *Traintracks Through Calabi-Yaus: Amplitudes Beyond Elliptic Polylogarithms*, [1805.09326](#).
- [55] J. L. Bourjaily, A. J. McLeod, C. Vergu, M. Volk, M. Von Hippel and M. Wilhelm, *Embedding Feynman Integral (Calabi-Yau) Geometries in Weighted Projective Space*, *JHEP* **01** (2020) 078, [[1910.01534](#)].
- [56] Z. Bern, J. Carrasco and H. Johansson, *New Relations for Gauge-Theory Amplitudes*, *Phys. Rev.* **D78** (2008) 085011, [[0805.3993](#)].
- [57] Z. Bern, J. J. M. Carrasco and H. Johansson, *Perturbative Quantum Gravity as a Double Copy of Gauge Theory*, *Phys. Rev. Lett.* **105** (2010) 061602, [[1004.0476](#)].
- [58] Z. Bern, J. J. M. Carrasco, M. Chiodaroli, H. Johansson and R. Roiban, *The Duality Between Color and Kinematics and its Applications*, [1909.01358](#).
- [59] T. Adamo, J. J. M. Carrasco, M. Carrillo-González, M. Chiodaroli, H. Elvang, H. Johansson, D. O’Connell et al., *Snowmass White Paper: the Double Copy and its Applications*, in *Snowmass 2021*, 4, 2022, [2204.06547](#).
- [60] Z. Bern, J. J. M. Carrasco, M. Chiodaroli, H. Johansson and R. Roiban, *Supergravity Amplitudes, the Double Copy and Ultraviolet Behavior*, [2304.07392](#).
- [61] N. E. J. Bjerrum-Bohr, P. H. Damgaard, T. Sondergaard and P. Vanhove, *The Momentum Kernel of Gauge and Gravity Theories*, *JHEP* **01** (2011) 001, [[1010.3933](#)].
- [62] C. R. Mafra, O. Schlotterer and S. Stieberger, *Explicit BCJ Numerators from Pure Spinors*, *JHEP* **07** (2011) 092, [[1104.5224](#)].
- [63] N. E. J. Bjerrum-Bohr, J. L. Bourjaily, P. H. Damgaard and B. Feng, *Manifesting Color-Kinematics Duality in the Scattering Equation Formalism*, *JHEP* **09** (2016) 094, [[1608.00006](#)].
- [64] S. Mizera, *Inverse of the String Theory KLT Kernel*, *JHEP* **06** (2017) 084, [[1610.04230](#)].
- [65] S. Mizera, *Kinematic Jacobi Identity is a Residue Theorem: Geometry of Color-Kinematics Duality for Gauge and Gravity Amplitudes*, *Phys. Rev. Lett.* **124** (2020) 141601, [[1912.03397](#)].
- [66] J. J. M. Carrasco, M. Chiodaroli, M. Günaydin and R. Roiban, *One-Loop Four-Point Amplitudes in Pure and Matter-Coupled $\mathcal{N} \leq 4$ Supergravity*, *JHEP* **03** (2013) 056, [[1212.1146](#)].

- [67] N. E. J. Bjerrum-Bohr, T. Dennen, R. Monteiro and D. O’Connell, *Integrand Oxidation and One-Loop Colour-Dual Numerators in $\mathcal{N}=4$ Gauge Theory*, *JHEP* **1307** (2013) 092, [[1303.2913](#)].
- [68] R. Monteiro and D. O’Connell, *The Kinematic Algebras from the Scattering Equations*, *JHEP* **1403** (2014) 110, [[1311.1151](#)].
- [69] S. He, R. Monteiro and O. Schlotterer, *String-Inspired BCJ Numerators for One-Loop MHV Amplitudes*, *JHEP* **01** (2016) 171, [[1507.06288](#)].
- [70] G. Mogull and D. O’Connell, *Overcoming Obstacles to Colour-Kinematics Duality at Two Loops*, *JHEP* **12** (2015) 135, [[1511.06652](#)].
- [71] H. Johansson, G. Kälin and G. Mogull, *Two-Loop Supersymmetric QCD and Half-Maximal Supergravity Amplitudes*, *JHEP* **09** (2017) 019, [[1706.09381](#)].
- [72] Z. Bern, J. J. M. Carrasco, W.-M. Chen, H. Johansson and R. Roiban, *Gravity Amplitudes as Generalized Double Copies of Gauge-Theory Amplitudes*, *Phys. Rev. Lett.* **118** (2017) 181602, [[1701.02519](#)].
- [73] A. Edison, S. He, H. Johansson, O. Schlotterer, F. Teng and Y. Zhang, *Perfecting One-Loop BCJ Numerators in SYM and Supergravity*, *JHEP* **02** (2023) 164, [[2211.00638](#)].
- [74] F. Porkert and O. Schlotterer, *One-Loop Amplitudes in Einstein-Yang-Mills from Forward Limits*, *JHEP* **02** (2023) 122, [[2201.12072](#)].
- [75] R. Monteiro and D. O’Connell, *The Kinematic Algebra From the Self-Dual Sector*, *JHEP* **07** (2011) 007, [[1105.2565](#)].
- [76] N. E. J. Bjerrum-Bohr, P. H. Damgaard, R. Monteiro and D. O’Connell, *Algebras for Amplitudes*, *JHEP* **06** (2012) 061, [[1203.0944](#)].
- [77] G. Chen, H. Johansson, F. Teng and T. Wang, *On the Kinematic Algebra for BCJ Numerators beyond the MHV Sector*, *JHEP* **11** (2019) 055, [[1906.10683](#)].
- [78] L. Borsten, B. Jurčo, H. Kim, T. Macrelli, C. Saemann and M. Wolf, *Becchi-Rouet-Stora-Tyutin-Lagrangian Double Copy of Yang-Mills Theory*, *Phys. Rev. Lett.* **126** (2021) 191601, [[2007.13803](#)].
- [79] N. Ahmadinia, F. M. Balli, O. Corradini, C. Lopez-Arcos, A. Q. Velez and C. Schubert, *Manifest Colour-Kinematics Duality and Double-Copy in the String-Based Formalism*, *Nucl. Phys. B* **975** (2022) 115690, [[2110.04853](#)].
- [80] M. Godazgar, C. N. Pope, A. Saha and H. Zhang, *BRST Symmetry and the Convolutional Double Copy*, *JHEP* **11** (2022) 038, [[2208.06903](#)].

- [81] R. Bonezzi, C. Chiaffrino, F. Diaz-Jaramillo and O. Hohm, *Gauge Invariant Double Copy of Yang-Mills Theory: The Quartic Theory*, *Phys. Rev. D* **107** (2023) 126015, [[2212.04513](#)].
- [82] R. Roiban, M. Spradlin and A. Volovich, *On the Tree-Level S-Matrix of Yang-Mills Theory*, *Phys. Rev.* **D70** (2004) 026009, [[hep-th/0403190](#)].
- [83] R. Britto, F. Cachazo and B. Feng, *New Recursion Relations for Tree Amplitudes of Gluons*, *Nucl.Phys.* **B715** (2005) 499–522, [[hep-th/0412308](#)].
- [84] R. Britto, F. Cachazo, B. Feng and E. Witten, *Direct Proof of Tree-Level Recursion Relation in Yang-Mills Theory*, *Phys. Rev. Lett.* **94** (2005) 181602, [[hep-th/0501052](#)].
- [85] J. Bedford, A. Brandhuber, B. J. Spence and G. Travaglini, *A Recursion Relation for Gravity Amplitudes*, *Nucl. Phys. B* **721** (2005) 98–110, [[hep-th/0502146](#)].
- [86] F. Cachazo and P. Svrcek, *Tree Level Recursion Relations in General Relativity*, [hep-th/0502160](#).
- [87] P. Benincasa, C. Boucher-Veronneau and F. Cachazo, *Taming Tree Amplitudes In General Relativity*, *JHEP* **11** (2007) 057, [[hep-th/0702032](#)].
- [88] N. E. J. Bjerrum-Bohr, D. C. Dunbar, H. Ita, W. B. Perkins and K. Risager, *MHV-Vertices for Gravity Amplitudes*, *JHEP* **01** (2006) 009, [[hep-th/0509016](#)].
- [89] M. Spradlin, A. Volovich and C. Wen, *Three Applications of a Bonus Relation for Gravity Amplitudes*, *Phys. Lett. B* **674** (2009) 69–72, [[0812.4767](#)].
- [90] H. Elvang and D. Z. Freedman, *Note on Graviton MHV amplitudes*, *JHEP* **05** (2008) 096, [[0710.1270](#)].
- [91] J. M. Drummond, M. Spradlin, A. Volovich and C. Wen, *Tree-Level Amplitudes in $\mathcal{N}=8$ Supergravity*, *Phys. Rev.* **D79** (2009) 105018, [[0901.2363](#)].
- [92] L. J. Mason and D. Skinner, *Gravity, Twistors and the MHV Formalism*, *Commun. Math. Phys.* **294** (2010) 827–862, [[0808.3907](#)].
- [93] F. A. Berends, W. T. Giele and H. Kuijf, *On Relations Between multi-Gluon and multi-Graviton Scattering*, *Phys. Lett. B* **211** (1988) 91–94.
- [94] Z. Bern, D. C. Dunbar and T. Shimada, *String Based Methods in Perturbative Gravity*, *Phys. Lett. B* **312** (1993) 277–284, [[hep-th/9307001](#)].
- [95] Z. Bern and A. K. Grant, *Perturbative Gravity from QCD Amplitudes*, *Phys. Lett. B* **457** (1999) 23–32, [[hep-th/9904026](#)].
- [96] S. Giombi, R. Ricci, D. Robles-Llana and D. Trancanelli, *A Note on Twistor Gravity Amplitudes*, *JHEP* **07** (2004) 059, [[hep-th/0405086](#)].

- [97] V. P. Nair, *A Note on MHV Amplitudes for Gravitons*, *Phys. Rev. D* **71** (2005) 121701, [[hep-th/0501143](#)].
- [98] N. Arkani-Hamed, J. L. Bourjaily, F. Cachazo, A. B. Goncharov, A. Postnikov and J. Trnka, *Grassmannian Geometry of Scattering Amplitudes*. Cambridge University Press, 2016, [10.1017/CBO9781316091548](#).
- [99] P. Heslop and A. E. Lipstein, *On-Shell Diagrams for $\mathcal{N}=8$ Supergravity Amplitudes*, [1604.03046](#).
- [100] E. Herrmann and J. Trnka, *Gravity On-shell Diagrams*, *JHEP* **11** (2016) 136, [[1604.03479](#)].
- [101] S. Paranjape, J. Trnka and M. Zheng, *Non-Planar BCFW Grassmannian Geometries*, *JHEP* **12** (2022) 084, [[2208.02262](#)].
- [102] J. Trnka, *Towards the Gravituhedron: New Expressions for NMHV Gravity Amplitudes*, *JHEP* **04** (2021) 253, [[2012.15780](#)].
- [103] T. V. Brown, U. Oktem and J. Trnka, *Poles at Infinity in On-Shell Diagrams*, *JHEP* **02** (2023) 003, [[2212.06840](#)].
- [104] J. L. Bourjaily, E. Gardi, A. J. McLeod and C. Vergu, *All-Mass n -gon Integrals in n Dimensions*, *JHEP* **08** (2020) 029, [[1912.11067](#)].
- [105] Z. Bern and A. G. Morgan, *Massive Loop Amplitudes from Unitarity*, *Nucl. Phys.* **B467** (1996) 479–509, [[hep-ph/9511336](#)].
- [106] R. Britto, F. Cachazo and B. Feng, *Computing One-Loop Amplitudes from the Holomorphic Anomaly of Unitarity Cuts*, *Phys. Rev.* **D71** (2005) 025012, [[hep-th/0410179](#)].
- [107] S. J. Bidder, N. E. J. Bjerrum-Bohr, D. C. Dunbar and W. B. Perkins, *One-Loop Gluon Acattering Amplitudes in Theories with $\mathcal{N} < 4$ Supersymmetries*, *Phys. Lett. B* **612** (2005) 75–88, [[hep-th/0502028](#)].
- [108] C. Anastasiou, R. Britto, B. Feng, Z. Kunszt and P. Mastrolia, *D-Dimensional Unitarity Cut Method*, *Phys. Lett.* **B645** (2007) 213–216, [[hep-ph/0609191](#)].
- [109] G. Ossola, C. G. Papadopoulos and R. Pittau, *Reducing Full One-Loop Amplitudes to Scalar Integrals at the Integrand Level*, *Nucl. Phys.* **B763** (2007) 147–169, [[hep-ph/0609007](#)].
- [110] L. J. Dixon, *Calculating Scattering Amplitudes Efficiently*, [hep-ph/9601359](#).
- [111] Z. Bern and Y.-t. Huang, *Basics of Generalized Unitarity*, *J. Phys.* **A44** (2011) 454003, [[1103.1869](#)].
- [112] H. Elvang and Y.-t. Huang, *Scattering Amplitudes*, [1308.1697](#).

- [113] M. B. Green, J. H. Schwarz and L. Brink, $\mathcal{N}=4$ Yang-Mills and $\mathcal{N}=8$ Supergravity as Limits of String Theories, *Nucl. Phys.* **B198** (1982) 474–492.
- [114] Z. Bern and D. A. Kosower, *The Computation of Loop Amplitudes in Gauge Theories*, *Nucl. Phys. B* **379** (1992) 451–561.
- [115] Z. Bern, *A Compact Representation of the One Loop n Gluon Amplitude*, *Phys. Lett. B* **296** (1992) 85–94.
- [116] Z. Bern, L. J. Dixon, M. Perelstein and J. Rozowsky, *Multileg One Loop Gravity Amplitudes from Gauge Theory*, *Nucl. Phys.* **B546** (1999) 423–479, [[hep-th/9811140](#)].
- [117] Z. Bern, N. E. J. Bjerrum-Bohr and D. C. Dunbar, *Inherited Swistor-Space Structure of Gravity Loop Amplitudes*, *JHEP* **05** (2005) 056, [[hep-th/0501137](#)].
- [118] N. E. J. Bjerrum-Bohr, D. C. Dunbar, H. Ita, W. B. Perkins and K. Risager, *The No-Triangle Hypothesis for $\mathcal{N}=8$ Supergravity*, *JHEP* **12** (2006) 072, [[hep-th/0610043](#)].
- [119] J. L. Bourjaily, C. Langer and Y. Zhang, *Illustrations of Integrand-Basis Building at Two Loops*, *JHEP* **08** (2022) 176, [[2112.05157](#)].
- [120] V. Del Duca, L. J. Dixon and F. Maltoni, *New Color Decompositions for Gauge Amplitudes at Tree and Loop Level*, *Nucl. Phys.* **B571** (2000) 51–70, [[hep-ph/9910563](#)].
- [121] A. Ochirov and B. Page, *Full colour for loop amplitudes in yang-mills theory*, *JHEP* **100** (02, 2017) .
- [122] J. L. Bourjaily, S. Franco, D. Galloni and C. Wen, *Stratifying On-Shell Cluster Varieties: the Geometry of Non-Planar On-Shell Diagrams*, *JHEP* **10** (2016) 003, [[1607.01781](#)].
- [123] E. Herrmann and J. Parra-Martinez, *Logarithmic forms and differential equations for feynman integrals*, .
- [124] A. V. Kotikov, *Differential Equations Method: New Technique for Massive Feynman Diagrams Calculation*, *Phys. Lett.* **B254** (1991) 158–164.
- [125] A. V. Kotikov, *The differential equation method: Evaluation of complicated feynman integrals*, 2000, [[hep-ph/0011316](#)].
- [126] E. Remiddi, *Differential Equations for Feynman Graph Amplitudes*, *Nuovo Cim.* **A110** (1997) 1435–1452, [[hep-th/9711188](#)].
- [127] J. L. Bourjaily, A. J. McLeod, M. von Hippel and M. Wilhelm, *Rationalizing Loop Integration*, *JHEP* **08** (2018) 184, [[1805.10281](#)].

- [128] J. L. Bourjaily, F. Dulat and E. Panzer, *Manifestly Dual-Conformal Loop Integration*, *Nucl. Phys.* **B942** (2019) 251–302, [[1901.02887](#)].
- [129] J. L. Bourjaily, M. Volk and M. Von Hippel, *Conformally Regulated Direct Integration of the Two-Loop Heptagon Remainder*, *JHEP* **02** (2020) 095, [[1912.05690](#)].
- [130] T. Becher and M. Neubert, *Infrared singularities of scattering amplitudes in perturbative qcd*, *PhysRevLett* **102** (2009) .
- [131] S. Catani, *The Singular Behavior of QCD Amplitudes at Two Loop Order*, *Phys. Lett.* **B427** (1998) 161–171, [[hep-ph/9802439](#)].
- [132] J. M. Henn, S. G. Naculich, H. J. Schnitzer and M. Spradlin, *Higgs-Regularized Three-Loop Four-Gluon Amplitude in $\mathcal{N}=4$ SYM: Exponentiation and Regge Limits*, *JHEP* **04** (2010) 038, [[1001.1358](#)].
- [133] J. M. Henn, S. G. Naculich, H. J. Schnitzer and M. Spradlin, *More Loops and Legs in Higgs-Regulated $\mathcal{N}=4$ SYM Amplitudes*, *JHEP* **08** (2010) 002, [[1004.5381](#)].
- [134] B. L. van der Waerden, *Spinoranalyse*, *Nach. Ges. Wiss. Göttingen Math.-Phys.* **1** (1929) 100–109.
- [135] N. Arkani-Hamed and J. Kaplan, *On Tree Amplitudes in Gauge Theory and Gravity*, *JHEP* **0804** (2008) 076, [[0801.2385](#)].
- [136] T. Cohen, H. Elvang and M. Kiermaier, *On-Shell Constructibility of Tree Amplitudes in General Field Theories*, *JHEP* **1104** (2011) 053, [[1010.0257](#)].
- [137] N. Arkani-Hamed, F. Cachazo and J. Kaplan, *What is the Simplest Quantum Field Theory?*, *JHEP* **1009** (2010) 016, [[0808.1446](#)].
- [138] S. J. Parke and T. R. Taylor, *An Amplitude for n -Gluon Scattering*, *Phys. Rev. Lett.* **56** (1986) 2459.
- [139] A. Hodges, *New Expressions for Gravitational Scattering Amplitudes*, *JHEP* **07** (2013) 075, [[1108.2227](#)].
- [140] H. Kawai, D. Lewellen and S. Tye, *A Relation Between Tree Amplitudes of Closed and Open Strings*, *Nucl. Phys.* **B269** (1986) 1.
- [141] J. L. Bourjaily, N. Kalyanapuram, K. Patatoukos, M. Plesser and Y. Zhang, “On-Shell Structure of Gravitational Tree Amplitudes.”
- [142] J. L. Bourjaily, N. Kalyanapuram, K. Patatoukos, M. Plesser and Y. Zhang, “Tools for Tree Amplitudes in Gauge Theory and Gravity.”
- [143] J. L. Bourjaily, *Efficient Tree-Amplitudes in $\mathcal{N}=4$: Automatic BCFW Recursion in MATHEMATICA*, [1011.2447](#).

- [144] J. M. H. P. W. Y. Z. D. Chicherin, T. Gehrmann and S. Zoia, *Analytic result for a two-loop five-particle amplitude*, *Phys. Rev. Lett* **122** (2019) .
- [145] E. H. B. P. S. Abreu, L. J. Dixon and M. Zeng, *The two-loop five-point amplitude in $\mathcal{N}=4$ super-yang-mills theory*, *Phys. Rev. Lett* **122** (2019) 121603.
- [146] E. H. B. P. S. Abreu, L. J. Dixon and M. Zeng, *The two-loop five-point amplitude in $\mathcal{N}=8$ supergravity*, *JHEP* **115** (03, 2019) .
- [147] J. M. H. P. W. Y. Z. D. Chicherin, T. Gehrmann and S. Zoia, *The two-loop five-particle amplitude in $\mathcal{N}=8$ supergravity*, *JHEP* **115** (03, 2019) .
- [148] Z. Bern, T. Dennen, Y.-t. Huang and M. Kiermaier, *Gravity as the Square of Gauge Theory*, *Phys. Rev.* **D82** (2010) 065003, [[1004.0693](#)].
- [149] S. H. Henry Tye and Y. Zhang, *Dual Identities Inside the Gluon and the Graviton Scattering Amplitudes*, *JHEP* **06** (2010) 071, [[1003.1732](#)].
- [150] Z. Bern, J. Carrasco, L. J. Dixon, H. Johansson and R. Roiban, *Simplifying Multiloop Integrands and Ultraviolet Divergences of Gauge Theory and Gravity Amplitudes*, *Phys. Rev.* **D85** (2012) 105014, [[1201.5366](#)].

Vita

Yaqi Zhang

Ph.D. candidates of Natural Science, Theoretical Physics
Penn State

2018-Current

Theoretical Physics
Central China Normal University

2016-2018

Bachelor of Natural Science, Theoretical Physics
Central China Normal University

2012-2016